

# Journal of Visualized Experiments

## Cell cycle-specific measurement of $\gamma$ H2AX and apoptosis after genotoxic stress by flow cytometry

--Manuscript Draft--

Article Type:	Invited Methods Article - JoVE Produced Video
Manuscript Number:	JoVE59968R2
Full Title:	Cell cycle-specific measurement of $\gamma$ H2AX and apoptosis after genotoxic stress by flow cytometry
Keywords:	DNA double-strand breaks; cell cycle distribution; apoptosis; DNA damage response; ionizing radiation; carbon ion radiation; genotoxic stress; flow cytometry, $\gamma$ H2AX
Corresponding Author:	Ramon Lopez Perez Deutsches Krebsforschungszentrum Heidelberg, GERMANY
Corresponding Author's Institution:	Deutsches Krebsforschungszentrum
Corresponding Author E-Mail:	r.lopez@dkfz-heidelberg.de
Order of Authors:	Ramon Lopez Perez Franziska Münz Jonas Kroschke Nils H. Nicolay Peter E. Huber
Additional Information:	
Question	Response
Please indicate whether this article will be Standard Access or Open Access.	Standard Access (US\$2,400)
Please indicate the <b>city, state/province, and country</b> where this article will be <b>filmed</b> . Please do not use abbreviations.	Heidelberg, Baden-Württemberg, Germany

German Cancer Research Center | E055 | PO Box 101949 | 69009 Heidelberg | Germany

Dr. DSouza, Senior Review Editor  
JoVE  
1 Alewife Center, Suite 200  
Cambridge, MA 02140

CCU  
Molecular and Radiation Oncology  
**Imaging and Radiooncology**  
E055  
Head:  
Peter Huber MD, PhD  
Professor of Radiation Oncology

Im Neuenheimer Feld 280  
69120 Heidelberg  
Germany  
Phone +49 6221 42-2516  
Telefax +49 6221 42-2442  
p.huber@dkfz.de  
www.dkfz.de

Heidelberg, 06/05/2019

## **Revision of Invited Manuscript 59968\_R0**

Dear Dr. DSouza:

Thank you for giving us the opportunity to submit a revised version of our invited manuscript to JoVE. We have carefully read and addressed the reviewer suggestions as well as the editorial comments. Besides editorial changes in the text, much more details were added to the protocol, particularly for software work, 2 new figures were added and the table of materials was updated.

We believe that the presented method can create a lot of interest in the audience of JoVE and hope that you find the revised manuscript acceptable for publication.

Yours sincerely,  
Ramon Lopez Perez

Ramon Lopez Perez, PhD  
CCU Molecular and Radiation Oncology  
Imaging and Radiooncology  
German Cancer Research Center  
Im Neuenheimer Feld 280  
69120 Heidelberg  
Germany  
Phone: +49 6221 42-2617  
r.lopez@dkfz.de

### **Foundation under Public Law**

Management Board  
Prof. Dr. med. Michael Baumann  
Prof. Dr. rer. pol. Josef Puchta

Deutsche Bank Heidelberg  
IBAN: DE09 6727 0003 0015 7008 00  
BIC (SWIFT): DEUT DES M672

Deutsche Bundesbank Karlsruhe  
IBAN: DE39 6600 0000 0067 0019 02  
BIC (SWIFT): MARK DEF 1660

**TITLE:**

Cell Cycle-Specific Measurement of  $\gamma$ H2AX and Apoptosis after Genotoxic Stress by Flow Cytometry

**AUTHORS & AFFILIATIONS:**

Ramon Lopez Perez<sup>1</sup>, Franziska Münz<sup>1</sup>, Jonas Kroschke<sup>1</sup>, Jannek Brauer<sup>1</sup>, Nils H. Nicolay<sup>1,2</sup>, Peter E. Huber<sup>1</sup>

<sup>1</sup>CCU Molecular and Radiation Oncology, German Cancer Research Center and Department of Radiation Oncology, Heidelberg University Hospital, Heidelberg, 69120, Germany

<sup>2</sup>Department of Radiation Oncology, Freiburg University Medical Center, Freiburg, 79106, Germany

**Corresponding Author:**

Ramon Lopez Perez (r.lopez@dkfz-heidelberg.de)

**Email Addresses of Co-authors:**

Franziska Münz (muenz@stud.uni-heidelberg.de)

Jonas Kroschke (j.kroschke@icloud.com)

Jannek Brauer (j.kroschke@icloud.com)

Nils H. Nicolay (n.nicolay@dkfz-heidelberg.de)

Peter E. Huber (p.huber@dkfz.de)

**KEYWORDS:**

DNA double-strand breaks, cell cycle distribution, apoptosis, DNA damage response, ionizing radiation, carbon ion radiation, genotoxic stress, flow cytometry

**SHORT ABSTRACT:**

The presented method combines the quantitative analysis of DNA double-strand breaks (DSBs), cell cycle distribution and apoptosis to enable cell cycle-specific evaluation of DSB induction and repair as well as the consequences of repair failure.

**LONG ABSTRACT:**

The presented method or slightly modified versions have been devised to study specific treatment responses and side effects of various anti-cancer treatments as used in clinical oncology. It enables a quantitative and longitudinal analysis of the DNA damage response after genotoxic stress, as induced by radiotherapy and a multitude of anti-cancer drugs. The method covers all stages of the DNA damage response, providing endpoints for induction and repair of DNA double-strand breaks (DSBs), cell cycle arrest and cell death by apoptosis in case of repair failure. Combining these measurements provides information about cell cycle-dependent treatment effects and thus allows an in-depth study of the interplay between cellular proliferation and coping mechanisms against DNA damage. As the effect of many cancer therapeutics including chemotherapeutic agents and ionizing radiation is limited to or strongly varies according to specific cell cycle phases, correlative analyses rely on a robust and feasible

method to assess the treatment effects on the DNA in a cell cycle-specific manner. This is not possible with single-endpoint assays and an important advantage of the presented method. The method is not restricted to any particular cell line and has been thoroughly tested in a multitude of tumor and normal tissue cell lines. It can be widely applied as a comprehensive genotoxicity assay in many fields of oncology besides radio-oncology, including environmental risk factor assessment, drug screening and evaluation of genetic instability in tumor cells.

## **INTRODUCTION:**

The goal of oncology is to kill or to inactivate cancer cells without harming normal cells. Many therapies either directly or indirectly induce genotoxic stress in cancer cells, but also to some extent in normal cells. Chemotherapy or targeted drugs are often combined with radiotherapy to enhance the radiosensitivity of the irradiated tumor<sup>1-5</sup>, which allows for a reduction of the radiation dose to minimize normal tissue damage.

Ionizing radiation and other genotoxic agents induce different kinds of DNA damage, including base modifications, strand crosslinks and single- or double-strand breaks. DNA double-strand breaks (DSBs) are the most serious DNA lesions and their induction is key to the cell killing effect of ionizing radiation and various cytostatic drugs in radiochemotherapy. DSBs do not only harm the integrity of the genome, but also promote the formation of mutations<sup>6,7</sup>. Therefore, different DSB repair pathways, and mechanisms to eliminate irreparably damaged cells like apoptosis have developed during evolution. The entire DNA damage response (DDR) is regulated by a complex network of signaling pathways that reach from DNA damage recognition and cell cycle arrest to allow for DNA repair, to programmed cell death or inactivation in case of repair failure<sup>8</sup>.

The presented flow cytometric method has been developed to investigate the DDR after genotoxic stress in one comprehensive assay that covers DSB induction and repair, as well as consequences of repair failure. It combines the measurement of the widely applied DSB marker  $\gamma$ H2AX with analysis of the cell cycle and induction of apoptosis, using classical subG1 analysis and more specific evaluation of caspase-3 activation.

The combination of these endpoints in one assay not only reduces time, labor and cost expenses, but also enables cell cycle-specific measurement of DSB induction and repair, as well as caspase-3 activation. Such analyses would not be possible with independently conducted assays, but they are highly relevant for a comprehensive understanding of the DNA damage response after genotoxic stress. Many anti-cancer drugs, such as cytostatic compounds, are directed against dividing cells and their efficiency is strongly dependent on the cell cycle stage. The availability of different DSB repair processes is also dependent on the cell cycle stage and pathway choice which is critical for the repair accuracy, and in turn determines the fate of the cell<sup>9-12</sup>. In addition, cell cycle-specific measurement of DSB levels is more accurate than pooled analysis, because DSB levels are not only dependent on the dose of a genotoxic compound or radiation, but also on the DNA content of the cell.

The method has been used to compare the efficacy of different radiotherapies to overcome resistance mechanisms in glioblastoma<sup>13</sup> and to dissect the interplay between ionizing radiation

and targeted drugs in osteosarcoma<sup>14, 15</sup> and atypical teratoid rhabdoid cancers<sup>16</sup>. Additionally, the described method has been widely used to analyze side effects of radio- and chemotherapy on mesenchymal stem cells<sup>17–24</sup>, which are essential for the repair of treatment-induced normal tissue damage and have a potential application in regenerative medicine.

## PROTOCOL:

### 1. Preparation

1.1. Prepare  $\geq 1 \times 10^5$  cells/sample in any type of culture vessel as starting material.

1.1.1. For example, conduct a time-course experiment after exposure of U87 glioblastoma cells to ionizing radiation: Irradiate sub-confluent U87 cells in T25 flasks in triplicates for each time point. Choose early time-points (15 min up to 8 h after irradiation) to follow the kinetics of DSB repair ( $\gamma$ H2AX level) and late time points (24 h up to 96 h) to assess residual DSB levels, cell cycle effects and apoptosis.

NOTE: The protocol is not restricted to irradiation experiments or any specific cell line. It has been tested with numerous cell lines of all types, from different species and for various treatment conditions.

1.2. Prepare the following solutions including 10% excess volume.

1.2.1. Prepare 2 mL per sample of fixation solution composed of 4.5% paraformaldehyde (PFA) in phosphate-buffered saline (PBS). Prepare the solution fresh. Dilute PFA in PBS by heating to 80 °C with slow stirring under the fume hood. Cover the flask with aluminum foil to prevent heat loss. Let the solution cool to room temperature and adjust the final volume. Pass the solution through a folded cellulose filter, grade 3hw (see the **Table of Materials**).

CAUTION: PFA fumes are toxic. Perform this step under a fume hood and dispose PFA waste appropriately.

1.2.2. Prepare 3 mL per sample of permeabilization solution composed of 70% ethanol in ice-cold H<sub>2</sub>O. Store at -20 °C.

1.2.3. Prepare 7 mL (per sample) of washing solution composed of 0.5% bovine serum albumin (BSA) in PBS.

1.2.4. Prepare 100  $\mu$ L per sample of 3% BSA in PBS as antibody diluent.

1.2.5. Prepare 100–250  $\mu$ L per sample of DNA staining solution composed of 1  $\mu$ g/mL 4',6-diamidin-2-phenylindol (DAPI) in PBS.

1.3. Set the centrifuge for 15 mL tubes to 5 min at 200 x *g* and 7 °C. Let the centrifuge cool down

and use these settings for all centrifugation steps.

## 2. Sample collection

2.1. If processing adherent cells (e.g., U87 glioblastoma cells grown in T25 flasks with 5 mL of Dulbecco's modified Eagle's medium supplemented with 10% fetal bovine serum at 37 °C and 5% carbon dioxide atmosphere), continue with steps 2.1.1. and 2.1.2. For suspension cells proceed directly to step 2.1.2.

2.1.1. Collect the medium in a centrifugation tube. Detach the cells using a routine cell culture method, which may include the use of trypsin, ethylenediaminetetraacetic acid (EDTA) or other cell detachment agents.

2.1.1.1. For U87 cells, prewarm PBS and trypsin/EDTA (see the **Table of Materials**) to 37 °C, wash the cell layer with 1 mL of PBS, incubate the cells for 1–2 min with 1 mL of trypsin/EDTA and support cell detachment by tapping at the flask. Collect all washing solution and the cell suspension in the tube with the medium.

2.1.2. Centrifuge the cells, discard the medium and resuspend the cells in 1 mL of PBS.

2.2. Pipet the cells up and down several times to ensure a single cell suspension and transfer the cell suspension into a tube with 2 mL of fixation solution (4.5% PFA/PBS, 3% final concentration).

CAUTION: PFA fumes are toxic. Perform this step under a fume hood and dispose PFA waste appropriately.

2.3. Incubate the cells for 10 min at room temperature.

2.4. Centrifuge the cells and discard the supernatant by decantation.

2.5. Loosen the cell pellet by tapping onto the tube and resuspend the cells in 3 mL of 70% ethanol. Proceed directly with the next step or store the samples at 4 °C for up to several weeks.

## 3. Washing and staining

3.1. Centrifuge the cells and discard the supernatant by decantation.

3.2. Loosen the cell pellet by tapping onto the tube. Resuspend the cells in 3 mL of washing solution (0.5% BSA/PBS), centrifuge and discard the supernatant.

3.3. Repeat the washing step 1x with 3 mL, and then 1x with 1 mL washing solution. In the last step, discard the supernatant **carefully** by pipetting. Take care not to aspirate the pellet.

3.4. Dilute the antibodies against  $\gamma$ H2AX, phospho-histone H3 (Ser10) and caspase-3 (see the

**Table of Materials**) in 100 µL/sample with antibody diluent (3% BSA/PBS).

3.5. Loosen the cell pellet by tapping onto the tube and resuspend the cells in 100 µL of the antibody solution prepared in step 3.4. Keep the samples in the dark from this step onward.

3.6. Incubate the samples for 1 h at room temperature.

3.7. Centrifuge the cells and discard the supernatant **carefully** by pipetting. Take care not to aspirate the pellet.

3.8. Loosen the cell pellet by tapping onto the tube and resuspend the cells in 100–250 µL of DNA staining solution (1 µg/mL DAPI/PBS).

3.8.1. Use 100 µL if  $1\text{--}2 \times 10^5$  cells are present and increase the volume for higher cell numbers ( $250 \mu\text{L}$  for  $\geq 1 \times 10^6$  cells). Proceed directly with the next step or store the samples in the dark at 4 °C for up to 2 weeks.

NOTE: For some cell types optimizing the DAPI concentration can help to improve the separation of the cell cycle phases.

3.9. Pipet the samples through the cell strainer cap of a sample tube with a mesh pore size of 35 µm.

#### 4. Measurement

4.1. Place the samples on ice, start the flow cytometer (see the **Table of Materials**) configured with an optical setup according to **Table 1** and press the **Prime** button. If required, switch on the ultraviolet laser (355 nm wavelength) separately and set the power to 10 mW using the appropriate software.

4.2. Open the acquisition software (see **Table of Materials**), log in and create a new experiment by clicking the **New Experiment** button on the **Browser** toolbar.

4.3. Use the **Inspector** window to customize the name of the experiment and choose '5 Log Decades' for plot display.

4.4. Click the **New Specimen** button in the **Browser** toolbar and expand the new entry by clicking the '+' symbol at its left side to show the first **Tube**. Select the respective icon and type to rename the **Specimen** (e.g., cell type) and the **Tube** (sample identifier). Click the **Tube Pointer** of the first **Tube** (arrow-like symbol at its left) to turn it green (active).

4.5. Open the **Parameters** tab in the **Cytometer** window and choose the parameters according to **Table 1**. Delete all unnecessary parameters.

NOTE: the parameter names may vary depending on the custom presets (e.g., Cy3 instead of Alexa555). Make sure that the selection matches the optical filters and detectors in **Table 1**. The light paths of all fluorophores are fully independent in this setup and compensation of spectral overlap is not required; however, it might be necessary if another optical setup is used.

4.6. Open the **Worksheet** window and create plots according to **Figure 1**. Draw 2 dot plots and 4 histograms using the corresponding toolbar buttons and click the axis labels to choose the appropriate parameters (front scatter (FSC-A) versus side scatter (SSC-A), DAPI-W versus DAPI-A and a histogram for DAPI-A and each antibody-coupled fluorophore.

4.7. Attach a control sample to the cytometer and press the **Run** button on the instrument. Select the first tube in the **Browser** window of the software and click the **Acquire Data** button in the **Acquisition Dashboard**. Adjust the sample injection volume using the **Low**, **Mid** or **High** buttons and the **fine tuning wheel** on the instrument. Preferably work at **Low** setting, but try to acquire at least 100 events/second (see **Acquisition Dashboard**).

4.8. Adjust the detector voltages for FSC, SSC and DAPI in the **Parameters** tab of the **Inspector** window using the dot plots in **Figure 1** as a guideline. Switch to logarithmic scale for the FSC and SSC parameters if the cell population appears too dispersed on a linear scale.

4.9. Press the **Standby** button on the cytometer and continue with the worksheet setup in the software.

4.9.1. Use the **Polygon Gate** tool to define the **Cells** population in the FSC-A versus SSC-A plot and the **Rectangle Gate** tool to define the **SingleCells** population in the DAPI-W versus DAPI-A plot. Press **Ctrl + G** keys to show the **Population Hierarchy** and click on the default gate names to rename them.

4.9.2. Subsequently right-click on all histograms and choose **Show Populations | SingleCells** from the context menu.

4.10. Optimize the detector voltages for the antibody-coupled fluorophores to cover the full dynamic range by subsequently acquiring control and treated samples. Maximize the signal-to-noise ratio and avoid detector saturation. Make sure that the Alexa488 peak in the **SingleCells** population is neither truncated in the control nor the treated sample.

4.11. Press the **Standby** button on the cytometer and **optionally** perform steps 4.11.1–4.11.3 in the **Worksheet** window of the software to get a rough estimate of treatment effects during sample acquisition.

4.11.1. Select **SingleCells** in the **Population Hierarchy** and use the **Rectangle Gate** tool to define the G1 population in the DAPI-W versus DAPI-A plot. Right-click at the Alexa488 histogram and choose **Show Populations | G1** from the context menu.



4.11.2. Right-click at the Alexa488 histogram and choose **Create Statistics View** from the context menu. Right-click at the **Statistics View** and choose **Edit Statistics View**. Go to the **Statistics** tab and activate the checkbox for the median of the Alexa488 signal in the G1 population (deactivate all other options).

4.11.3. Select **SingleCells** in the **Population Hierarchy** and use the **Interval Gate** tool to define the **subG1**, **M** and **Casp3+** populations in the DAPI-A, Alexa555-A (Cy3-A in **Figure 1**) and Alexa647-A histograms.

4.12. Press the **Run** button on the cytometer and measure the samples using the **Acquisition Dashboard** in the software. Set the stopping gate to **All events** or the **Cells** gate (if numerous small particles are present) and the number of events to record to 10,000.

4.13. Click **Next Tube** to create a new sample, rename it in the **Browser** window, click **Acquire Data** to start the acquisition and **Record Data** to start recording.

4.14. Select **File | Export | Experiments** from the menu bar and choose **Directory Export** in the dialog box to save the data as '.fcs' files. Optionally save the experiment as an additional **zip file** if to enable reimporting the experiment at a later time point.

NOTE: The setup of existing experiments can be easily reused with **Edit | Duplicate without data**.

## 5. Data evaluation

5.1. Drag and drop the '.fcs' files into the sample browser of the flow cytometric analysis software (see **Table of Materials**). Apply the gating strategy shown in **Figure 2**. Make sure that the gates fit to the corresponding population in all of the samples before proceeding with the next daughter gate.

5.1.1. To apply changes to all samples, select the changed gate in the sample browser, copy it by pressing **Ctrl + C**, select the parent gate, press **Ctrl + Shift + E** to select the equivalent nodes in all samples and press **Ctrl + V** to paste or overwrite the gate. Do not use group gates.

5.1.2. Double-click on the first sample in the browser to open the SSC-A vs. FSC-A plot. Use the **Polygon** tool in the toolbar to define the **Cells** population (**Figure 2**, plot 1), excluding debris from the analysis. Make sure that the gate is wide enough towards the upper right corner to accommodate treatment-related shifts, but restrict the border facing to the lower left corner of the plot to reliably exclude the cell.

5.1.3. Double-click on the **Cells** gate to open a new plot window and change the axes to DAPI-W (vertical) vs. DAPI-A (horizontal) by clicking on the axis labels. Use the **Rectangle** tool to define the **SingleCells** population (**Figure 2**, plot 2), excluding cell doublets or clumps from the analysis (doublets of G1 cells have the same DAPI-A intensity as G2 and M cells, but a considerably higher DAPI-W value).

NOTE: Varying cell counts in different samples will cause shifts in the overall DAPI-A signal strength due to equilibrium binding of DAPI to DNA. This will not affect the cell cycle analysis, but it may be necessary to adjust the right border of the single cell gate sample by sample to account for these shifts.

5.1.4. Double-click on the **SingleCells** gate to open a new plot window and change the axes to show the DAPI-A histogram. Use the **Bisector** tool to distinguish single cells with normal DNA content (**CellCycle** population) from apoptotic cells with degraded DNA (**subG1** population). Subsequently select the new gates in the browser and press **Ctrl + R** to rename them accordingly (**Figure 2**, plot 3).

5.1.5. Select the **CellCycle** gate in the browser and choose **Tool | Biology | Cell Cycle...** from the menu bar to open the cell cycle modelling tool. Choose Dean-Jett-Fox<sup>25, 26</sup> in the **Model** section to estimate the frequency of cells in G1, S and G2/M phase (**Figure 2**, plot 4).

5.1.5.1. Use constraints only in case of poor modelling performance (minimize the **Root Mean Square** deviation between model and data).

5.1.6. Create gates for **G1** (**Ellipse** tool), **S** (**Polygon** tool) and **G2 + M** (**Ellipse** tool) phase in the DAPI-W vs. DAPI-A plot of the **CellCycle** population to enable cell cycle-specific  $\gamma$ H2AX measurement (**Figure 2**, plot 5).

5.1.6.1. Do not use the modelling tool for automatic cell cycle gating based on the DAPI-A histogram, as this can be inaccurate.

NOTE: It may be necessary to move the gates along the DAPI-A axis sample by sample to account for the aforementioned shifts in overall DAPI signal strength. Only move the three gates as a group and do not change the shape of individual gates to avoid bias.

5.1.7. Use the **Bisector** tool to distinguish phospho-histone H3-positive (**M**) and -negative (**M-**) cells in the Alexa555-A histogram of the **SingleCells** population (**Figure 2**, plot 6). Hold **Ctrl** and select the gates **G2 + M** and **M-**. Press **Ctrl + Shift + A** to create the **G2** (G2+M & M-) gate.

5.1.8. Use the **Bisector** tool to distinguish caspase-3-positive (**Casp3+**) and -negative (**Casp3-**) cells in the Alexa647-A histogram of the **SingleCells** population (**Figure 2**, plot 7). Set the threshold such that the average of the **Casp3+** population in the untreated controls amounts to ~0.8% to assure high sensitivity and minimize assay-to-assay variations.

5.1.9. Press **Ctrl + T** to open the **Table Editor** and configure it according to **Figure 3**. Drag and drop the different populations from the sample browser into the **Table Editor** and double-click on the rows to change the statistic, parameter and name settings. Remove the unnecessary rows that are automatically added after the drag and drop of the cell cycle modelling icon by selecting the rows and pressing **Del**.

5.1.10. Choose **To File**, the format and destination in the **Output** section of the menu ribbon and click **Create Table** to export the data as '.xlsx' file.

5.2. Use table calculation software (see **Table of Materials**) for further data analysis according to **Supplementary File 1** (FACS Analysis Template.xlsx).

5.2.1. Correct the frequencies of cells in the different cell cycle phases such that their sum amounts to 100% by applying the formula  $X' = X * 100 / \Sigma(\text{all cell cycle phases})$ , with X': corrected value, X: raw value, to each cell cycle phase.

NOTE: Deviations from a sum of 100% occur due to inaccuracies in the cell cycle modelling, but are usually small (<5%).

5.2.2. Normalize the median  $\gamma$ H2AX intensities to the DNA content in the different cell cycle phases by dividing the values in S phase by 1.5 and in G2 and M phase by 2.0.

5.2.3. To calculate the combined normalized  $\gamma$ H2AX level in the whole cell population, use the formula  $I_A = I_{G1} * G1 + I_S * S + I_{G2} * G2 + I_M * M$ , where  $I_A$ ,  $I_{G1}$ ,  $I_S$ ,  $I_{G2}$ ,  $I_M$  are normalized median  $\gamma$ H2AX intensities of all, G1, S, G2, M cells respectively and G1, S, G2, M are corrected frequency of cells in the respective cell cycle phase.

5.2.4. For the normalized  $\gamma$ H2AX levels and the frequency of subG1 and caspase-3-positive cells, subtract the average value of the untreated controls from each sample.

5.2.5. Calculate the mean and standard deviation of each parameter from all replicate samples and plot the results into diagrams.

## REPRESENTATIVE RESULTS:

Human U87 or LN229 glioblastoma cells were irradiated with 4 Gy of photon or carbon ion radiation. Cell cycle-specific  $\gamma$ H2AX levels and apoptosis were measured at different time points up to 48 h after irradiation using the flow cytometric method presented here (**Figure 3**). In both cell lines, carbon ions induced higher  $\gamma$ H2AX peak levels that declined slower and remained significantly elevated at 24 to 48 h compared to photon radiation at the same physical dose (**Figure 4A**). This indicated that carbon ions induced higher peak levels of DNA double-strand breaks (DSBs) than photons that were repaired less efficiently. For both radiation types, the  $\gamma$ H2AX levels were highest in G1 cells, probably because DSB repair is limited to the pathway of non-homologous end-joining at this stage of the cell cycle.

In line with the higher DSB induction rate and slower repair kinetics, carbon ions induced a stronger and longer-lasting cell cycle arrest in G2 phase (**Figure 3B**) and a higher rate of apoptosis than photons (**Figure 4C**). Carbon ion radiation may therefore help to overcome radioresistance mechanisms observed in glioblastoma upon classical radiotherapy with photons (see Lopez, et al.<sup>1</sup> for detailed discussion).

The results shown in **Figure 4** are examples of an optimal outcome of this method, showing clear differences between untreated and irradiated cells and statistically significant differential effects between different treatments. In cases where induction of DSBs and apoptosis is less clear, it is important to include positive controls. As shown here, cells fixed 1 h after photon irradiation are good positive controls for  $\gamma$ H2AX induction. Photon radiation is also known to efficiently induce apoptosis in lymphocytes, which makes them useful as positive controls for apoptosis 2-4 days after irradiation. Another possibility is to use drugs for apoptosis induction, such as the proteasome inhibitor MG132 or a death receptor ligand (**Figure 5**).

Another important aspect for an optimal outcome of the assay is the quality of the cell cycle profiles. In **Figure 4B** the G1 and G2 peaks were narrow and clearly separated, making it easy to apply cell cycle modelling and to define the gates for cell-cycle-specific measurement of  $\gamma$ H2AX. Depending on the cell type and the strength of the treatment effect (**Figure 6A,B**), the resolution of the different cell cycle phases can be significantly worse. In some cases, the DAPI concentration has a big impact on the quality of the cell cycle profile and needs to be adjusted (**Figure 6C**). In cases where no clear G1 peak is detectable due to the treatment, the cell cycle modelling tool cannot be applied accurately. It is advisable then to only use manual gating in the DAPI-A versus DAPI-W plot based on controls with a well-defined cell cycle profile, as described in the protocol. The analysis of a cell cycle profile without a clear G1 peak can be further complicated if the treatment leads to low cell numbers that result in large shifts in the overall DAPI signal strength. In this situation, it can be difficult to judge, if a peak is the G1 or the G2 peak. To avoid this problem, the cells can be counted with a Neubauer chamber or by other means after the last washing step (step 2.3) and the cell numbers can be adjusted. The peak positions in the treated cells will then match with the controls.

#### FIGURE AND TABLE LEGENDS:

**Figure 1: Worksheet setup for sample acquisition.** Plots and gates for signal display in the Worksheet window of the flow cytometer software (see the **Table of Materials**).

**Figure 2: Gating strategy for data evaluation.** Population tree and diagrams showing how the gates are set to define the different sub-populations in the flow cytometric analysis software. DJF refers to the cell cycle modelling tool using the Dean-Jett-Fox method<sup>25, 26</sup>.

**Figure 3: Raw data export table.** Setup of the 'Table Editor' for raw data export in the flow cytometric analysis software.

**Figure 4: DNA damage response of human U87 and LN229 glioblastoma cells after irradiation with 4 Gy of photon versus carbon ion radiation.** (A) DSB induction and repair measured by  $\gamma$ H2AX levels. The median fluorescence intensity was normalized to the relative DNA content in each cell cycle phase (G1 = 1.0, S = 1.5, G2 = 2.0) and control levels were subtracted. Symbols indicate mean and error bars indicate SD values. Solid lines represent fits according to the function  $I(t) = (p1*t^2 + p2*t) / (t^2 + q1*t + q2) \mid t \geq 0, p1 < 0, p1, q1, q2 > 0$ . (B) Cell cycle distribution

(mean and SD) and representative histograms of the DNA content marker DAPI at 24 h after photon or carbon ion irradiation. (C) Apoptosis induction, as measured by caspase-3 and subG1 positive cells (mean and SD). \*P < 0.05, \*\*P < 0.01, \*\*\*P < 0.001 (two-sided Student's t test). This figure has been modified from Lopez, et al.<sup>1</sup> with permission.

**Figure 5: Drug-mediated apoptosis-induction in U87 glioblastoma cells.** U87 cells were treated with 5 ng/mL of a modified TNF-related apoptosis-inducing ligand (see **Table of Materials**) plus 2.5  $\mu$ M MG132 for 20 h before fixation to validate the apoptosis measurement by active caspase-3 and subG1 analysis. (A) Histogram of the caspase-3 signal of treated versus untreated cells. (B) DAPI histogram of treated cells with a subG1 population, indicating DNA degradation. The histogram of caspase-3-positive events is overlaid in red, demonstrating that most of the apoptotic cells had not yet degraded their DNA at this time point.

**Figure 6: Factors influencing the quality of cell cycle profiles.** Too harsh treatments complicate cell cycle analysis. (A) No G1 peak is detectable 48 h after treatment of LLC cells (Lewis lung carcinoma) with 20 Gy of photon radiation or (B) 96 h after treatment of HS68 fibroblasts with 100 mJ of UV radiation. (C) DAPI concentration in different cell lines: In HS68 fibroblasts (upper panel) the G2/M peak (see arrows) was equally well-separated from the G1 peak for DAPI concentrations between 0.01 and 1.0  $\mu$ g/mL. In contrast, DAPI concentrations below 0.75  $\mu$ g/mL resulted in poor separation and shape definition of the G2/M peak (see arrows) in MRC-5 fibroblasts (lower panel).

**Table 1: Typical flow cytometer configuration.**  $\lambda$  = wavelength of the excitation laser, U = detector voltage, log = logarithmic scale (otherwise linear), -A = signal area, -H = maximum signal height, -W = signal width (duration), FSC = front scatter, SSC = side scatter. Optical filter specifications are given as central wavelength/bandwidth in nanometers. Settings may vary for different flow cytometers and detector voltages need to be adjusted for different cell lines.

**Supplementary Figure 1: Microscopic images of  $\gamma$ H2AX foci.** U87 cells were irradiated with different doses of photon radiation, fixed and stained after 30 min according to the presented protocol and prepared for microscopy as described in the discussion. At 2 Gy, individual foci could be easily distinguished, while at 8 Gy foci counting was biased due to considerable overlap.

## DISCUSSION:

The featured method is easy to use and offers a fast, accurate and reproducible measurement of the DNA damage response including double-strand break (DSB) induction and repair, cell cycle effects and apoptotic cell death. The combination of these endpoints provides a more complete picture of their interrelations than individual assays. The method can be widely applied as a comprehensive genotoxicity assay in the fields of radiation biology, therapy and protection, and more generally in oncology (e.g., for environmental risk factor assessment, drug screening and evaluation of genetic instability in tumor cells).

The most critical step in this protocol is the fixation of the cells. To obtain a clean sample with a clearly defined cell population and optimal resolution of different cell cycle phases, it is important

to give adherent cells enough time to detach from the culture vessel and form a completely round shape. The cells should be transferred into the fixation solution as a single cell suspension without cell clumps. To separate them, the cells must be pipetted up and down or passed through a fine needle several times in difficult cases. The fixation time should be kept constant between all samples and should not exceed 20 min including the time for centrifugation before resuspension of the cells in 70% ethanol. Prolonged fixation will lead to loss of accessible epitopes for antibody binding and will decrease the signal strength and sensitivity of the method.

The main limitation of the technique is that it does not provide information on the quality of the  $\gamma$ H2AX foci other than the intensity in the whole nucleus. Particularly large  $\gamma$ H2AX foci as well as the occurrence of a pan-nuclear  $\gamma$ H2AX staining have been linked to clustered DSBs<sup>1, 27–29</sup>, which are highly complex lesions are very difficult to repair<sup>30</sup>. Such clustered lesions seem to be characteristic of particle radiation such as clinically applied carbon ion radiation and may be the reason for the superior biological effectiveness of heavy ion radiation compared to photons<sup>31–33</sup>. Analysis of the  $\gamma$ H2AX foci size may therefore be of interest as an indicator of the damage complexity. Although it is possible to use the present protocol with an image stream cytometer to visualize the  $\gamma$ H2AX foci, the achievable resolution cannot compete with a classical microscopic approach. However, we have successfully prepared microscopic slides from the remaining samples after flow cytometric measurement (**Supplementary Figure 1**) and evaluated several features including  $\gamma$ H2AX foci count, size and pan-nuclear intensity using a semi-automated imaging and analysis system. To prepare the samples for microscopy, 30–50  $\mu$ L of the stained cells were spread over the surface of a 24 mm x 24 mm cover glass, air dried overnight at room temperature in the dark and then embedded with mounting medium on a glass slide.

In comparison with microscopic evaluation of DSB levels by  $\gamma$ H2AX foci counting, the flow cytometric measurement is superior in throughput, sampling rate, dynamic range and accuracy. The dynamic range of microscopic foci counting is limited by the optical resolution, leading to the inability to distinguish overlapping foci<sup>29, 34</sup>. In practice, we have observed a linear relationship between radiation dose and  $\gamma$ H2AX foci numbers below 2 Gy, and a strong saturation effect above 2 Gy in U87 glioblastoma cells<sup>1</sup>. In contrast, the intensity of the  $\gamma$ H2AX signal measured by flow cytometry increased linearly with dose for the whole dose range tested (0–8 Gy).

The accuracy of microscopic foci counting is limited by the inability to distinguish between different cell cycle phases without additional stainings<sup>35</sup>. The number of DSBs induced in a cell is not only dependent on the radiation dose, but also on the DNA content, and hence the cell cycle stage. G2 cells for example have twice as much DNA as G1 cells and the average number of DSBs induced at a certain radiation dose is twice as high for G2 cells compared to G1. This is clearly reflected in the  $\gamma$ H2AX signal intensity of G2 versus G1 cells at early time points after radiation measured by flow cytometry. Therefore, it is important to evaluate DSB levels in a cell cycle-specific manner to obtain accurate results. A pooled analysis of cells in different cell cycle phases, like usual in microscopic approaches, can be biased by shifts in the cell cycle distribution particularly due to radiation-induced G2 arrest. To account for this effect and to compare DSB repair characteristics between different cell cycle stages, the  $\gamma$ H2AX levels can easily be normalized to the DNA content in the flow cytometry method as indicated in the protocol.

Extensions of the present protocol are possible with relatively little extra effort. Additional antibodies with compatible fluorophores labels can be included in step 3.4 without the need for any extra steps during sample preparation. If a more detailed analysis of apoptosis is desired, caspase-7, -9 and -8 antibodies could be included. As another extension, we have recently included a live and dead cell dyes, a troponin T antibody and counting beads in the protocol to specifically analyze cardiomyocytes co-cultured with fibroblasts after irradiation. The addition of the live/dead cell stain and the counting beads expands the capability of the method to include fibroblast proliferation and non-apoptotic cell death of the cardiomyocytes as further endpoints that provide useful additional information on the cell fate after genotoxic stress. The extended protocol is available upon request.

#### ACKNOWLEDGMENTS:

We thank the Flow Cytometry Facility team at the German Cancer Research Center (DKFZ) for their support.

#### DISCLOSURES:

The authors have nothing to disclose.

#### REFERENCES:

Use the "Insert Citation" button to add citations to this document.

#### REFERENCES:

1. Jensen, A., et al. Treatment of non-small cell lung cancer with intensity-modulated radiation therapy in combination with cetuximab: the NEAR protocol (NCT00115518). *BMC Cancer*. **6**, 122, doi: 10.1186/1471-2407-6-122 (2006).
2. Oertel, S., et al. Human Glioblastoma and Carcinoma Xenograft Tumors Treated by Combined Radiation and Imatinib (Gleevec). *Strahlentherapie und Onkologie*. **182** (7), 400–407, doi: 10.1007/s00066-006-1445-8 (2006).
3. Timke, C., et al. Combination of Vascular Endothelial Growth Factor Receptor/Platelet-Derived Growth Factor Receptor Inhibition Markedly Improves Radiation Tumor Therapy. *Clinical Cancer Research*. **14** (7), 2210–2219, doi: 10.1158/1078-0432.CCR-07-1893 (2008).
4. Zhang, M., et al. Trimodal glioblastoma treatment consisting of concurrent radiotherapy, temozolomide, and the novel TGF- $\beta$  receptor I kinase inhibitor LY2109761. *Neoplasia*. **13** (6), 537–49 (2011).
5. Blattmann, C., et al. Suberoylanilide hydroxamic acid affects  $\gamma$ H2AX expression in osteosarcoma, atypical teratoid rhabdoid tumor and normal tissue cell lines after irradiation. *Strahlentherapie und Onkologie*. **188** (2), 168–176, doi: 10.1007/s00066-011-0028-5 (2012).
6. Hoeijmakers, J.H. DNA Damage, Aging, and Cancer. *New England Journal of Medicine*. **361** (15), 1475–1485, doi: 10.1056/NEJMr0804615 (2015).
7. Rodgers, K., McVey, M. Error-Prone Repair of DNA Double-Strand Breaks. *Journal of Cellular Physiology*. **231** (1), 15–24, doi: 10.1002/jcp.25053 (2016).
8. Ciccia, A., Elledge, S.J. The DNA Damage Response: Making It Safe to Play with Knives. *Molecular Cell*. **40** (2), 179–204, doi: 10.1016/j.molcel.2010.09.019 (2010).

- 573 9. Lopez Perez, R., et al. DNA damage response of clinical carbon ion versus photon radiation  
574 in human glioblastoma cells. *Radiotherapy and Oncology*. **133**, 77–86, doi:  
575 10.1016/j.radonc.2018.12.028 (2019).
- 576 10. Oertel, S., et al. Combination of suberoylanilide hydroxamic acid with heavy ion therapy  
577 shows promising effects in infantile sarcoma cell lines. *Radiation oncology*. **6** (1), 119, doi:  
578 10.1186/1748-717X-6-119 (2011).
- 579 11. Blattmann, C., et al. Suberoylanilide hydroxamic acid affects  $\gamma$ H2AX expression in  
580 osteosarcoma, atypical teratoid rhabdoid tumor and normal tissue cell lines after irradiation.  
581 *Strahlentherapie und Onkologie*. **188** (2), 168–176, doi: 10.1007/s00066-011-0028-5 (2012).
- 582 12. Thiemann, M., et al. In vivo efficacy of the histone deacetylase inhibitor suberoylanilide  
583 hydroxamic acid in combination with radiotherapy in a malignant rhabdoid tumor mouse model.  
584 *Radiation Oncology*. **7** (1), 52, doi: 10.1186/1748-717X-7-52 (2012).
- 585 13. Nicolay, N.H., et al. Mesenchymal stem cells retain their defining stem cell characteristics  
586 after exposure to ionizing radiation. *International Journal of Radiation Oncology Biology Physics*.  
587 **87** (5), 1171–1178, doi: 10.1016/j.ijrobp.2013.09.003 (2013).
- 588 14. Nicolay, N.H., et al. Mesenchymal stem cells are resistant to carbon ion radiotherapy.  
589 *Oncotarget*. **6** (4), 2076–87 (2015).
- 590 15. Nicolay, N.H., et al. Mesenchymal stem cells exhibit resistance to topoisomerase  
591 inhibition. *Cancer letters*. **374** (1), 75–84, doi: 10.1016/j.canlet.2016.02.007 (2016).
- 592 16. Nicolay, N.H., et al. Mesenchymal stem cells maintain their defining stem cell  
593 characteristics after treatment with cisplatin. *Scientific Reports*. **6** (January), 20035, doi:  
594 10.1038/srep20035 (2016).
- 595 17. Nicolay, N.H., et al. Mesenchymal stem cells are sensitive to bleomycin treatment.  
596 *Scientific Reports*. **6** (May), 26645, doi: 10.1038/srep26645 (2016).
- 597 18. Rühle, A., et al. Cisplatin radiosensitizes radioresistant human mesenchymal stem cells.  
598 *Oncotarget*. **8** (50), 87809–87820, doi: 10.18632/oncotarget.21214 (2017).
- 599 19. Münz, F., et al. Human mesenchymal stem cells lose their functional properties after  
600 paclitaxel treatment. *Scientific Reports*. **8** (1), 312, doi: 10.1038/s41598-017-18862-1 (2018).
- 601 20. Rühle, A., et al. The Radiation Resistance of Human Multipotent Mesenchymal Stromal  
602 Cells Is Independent of Their Tissue of Origin. *International Journal of Radiation Oncology Biology*  
603 *Physics*. **100** (5), 1259–1269, doi: 10.1016/j.ijrobp.2018.01.015 (2018).
- 604 21. Rothkamm, K., Krüger, I., Thompson, L.H., Löbrich, M. Pathways of DNA double-strand  
605 break repair during the mammalian cell cycle. *Molecular and Cellular Biology*. **23** (16), 5706–15,  
606 doi: 10.1128/mcb.23.16.5706-5715.2003 (2003).
- 607 22. Escribano-Díaz, C., et al. A Cell Cycle-Dependent Regulatory Circuit Composed of 53BP1-  
608 RIF1 and BRCA1-CtIP Controls DNA Repair Pathway Choice. *Molecular Cell*. **49** (5), 872–883, doi:  
609 10.1016/j.molcel.2013.01.001 (2013).
- 610 23. Bakr, A., et al. Functional crosstalk between DNA damage response proteins 53BP1 and  
611 BRCA1 regulates double strand break repair choice. *Radiotherapy and Oncology*. **119** (2), 276–81,  
612 doi: 10.1016/j.radonc.2015.11.001 (2015).
- 613 24. Mladenov, E., Magin, S., Soni, A., Iliakis, G. DNA double-strand-break repair in higher  
614 eukaryotes and its role in genomic instability and cancer: Cell cycle and proliferation-dependent  
615 regulation. *Seminars in Cancer Biology*. **37–38**, 51–64, doi: 10.1016/j.semcancer.2016.03.003  
616 (2016).



25. Dean, P.N., Jett, J.H. Mathematical analysis of DNA distributions derived from flow microfluorometry. *Journal of Cell Biology*. **60** (2), 523–527 (1974).
26. Fox, M.H. A model for the computer analysis of synchronous DNA distributions obtained by flow cytometry. *Cytometry*. **1** (1), 71–77, doi: 10.1002/cyto.990010114 (1980).
27. Costes, S. V, Boissière, A., Ravani, S., Romano, R., Parvin, B., Barcellos-Hoff, M.H. Imaging features that discriminate between foci induced by high- and low-LET radiation in human fibroblasts. *Radiation Research*. **165** (5), 505–515, doi: 10.1667/RR3538.1 (2006).
28. Meyer, B., Voss, K.-O., Tobias, F., Jakob, B., Durante, M., Taucher-Scholz, G. Clustered DNA damage induces pan-nuclear H2AX phosphorylation mediated by ATM and DNA-PK. *Nucleic Acids Research*. **41** (12), 6109–6118, doi: 10.1093/nar/gkt304 (2013).
29. Lopez Perez, R., et al. Superresolution light microscopy shows nanostructure of carbon ion radiation-induced DNA double-strand break repair foci. *FASEB*. **30** (8), 2767–2776, doi: 10.1096/fj.201500106R (2016).
30. Schipler, A., Iliakis, G. DNA double-strand-break complexity levels and their possible contributions to the probability for error-prone processing and repair pathway choice. *Nucleic Acids Research*. **41** (16), 7589–7605, doi: 10.1093/nar/gkt556 (2013).
31. Stenerlow, B., Hoglund, E., Carlsson, J. DNA fragmentation by charged particle tracks. *Advances in Space Research*. **30** (4), 859–863 (2002).
32. Friedland, W., et al. Comprehensive track-structure based evaluation of DNA damage by light ions from radiotherapy-relevant energies down to stopping. *Scientific Reports*. **7**, 45161, doi: 10.1038/srep45161 (2017).
33. Pang, D., Chasovskikh, S., Rodgers, J.E., Dritschilo, A. Short DNA Fragments Are a Hallmark of Heavy Charged-Particle Irradiation and May Underlie Their Greater Therapeutic Efficacy. *Frontiers in Oncology*. **6**, 130, doi: 10.3389/fonc.2016.00130 (2016).
34. Böcker, W., Iliakis, G. Computational Methods for analysis of foci: validation for radiation-induced gamma-H2AX foci in human cells. *Radiation Research*. **165** (1), 113–124 (2006).
35. Löbrich, M., et al.  $\gamma$ H2AX foci analysis for monitoring DNA double-strand break repair: Strengths, limitations and optimization. *Cell Cycle*. **9** (4), 662–669, doi: 10.4161/cc.9.4.10764 (2010).

# Figure 1

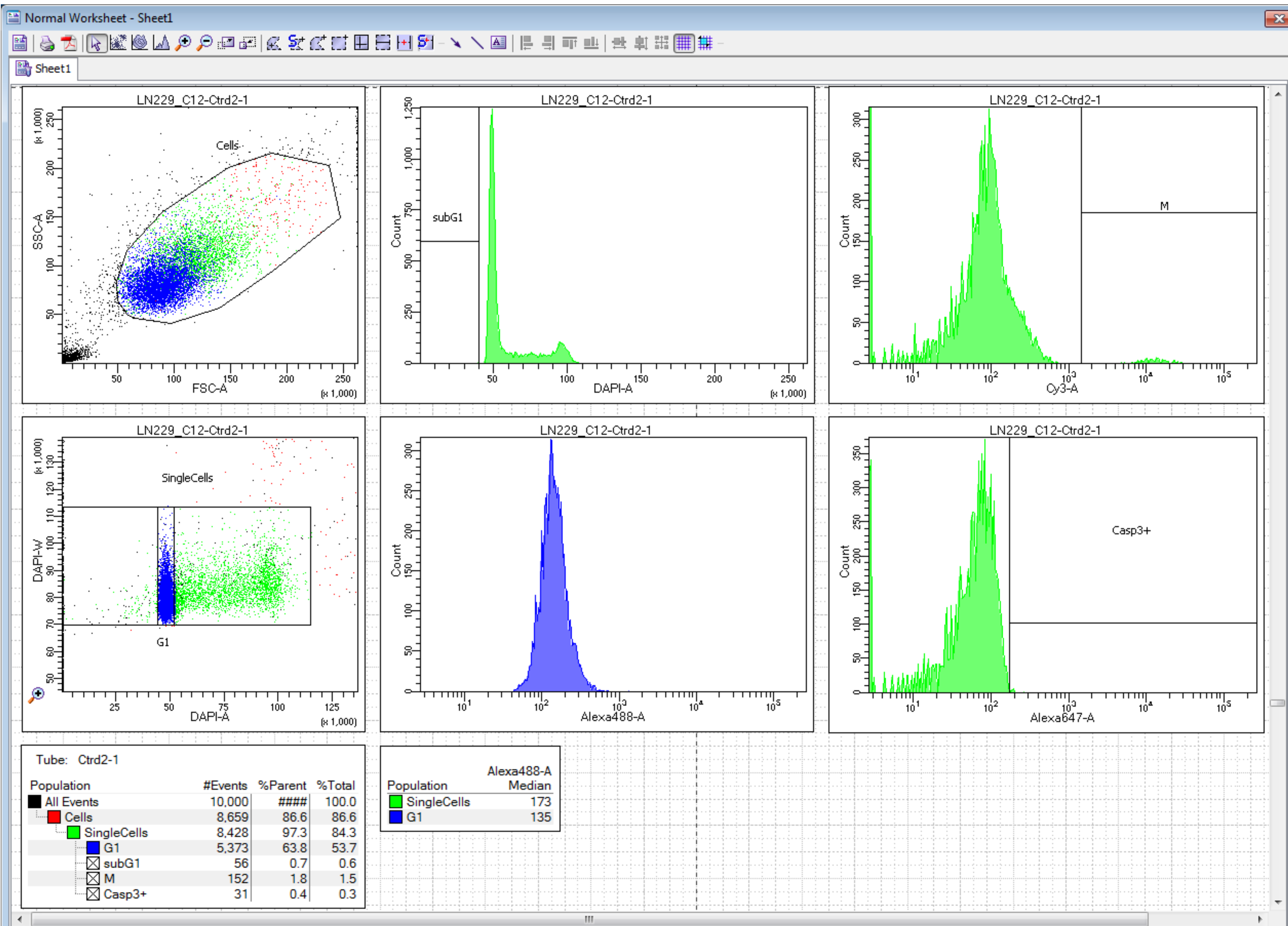
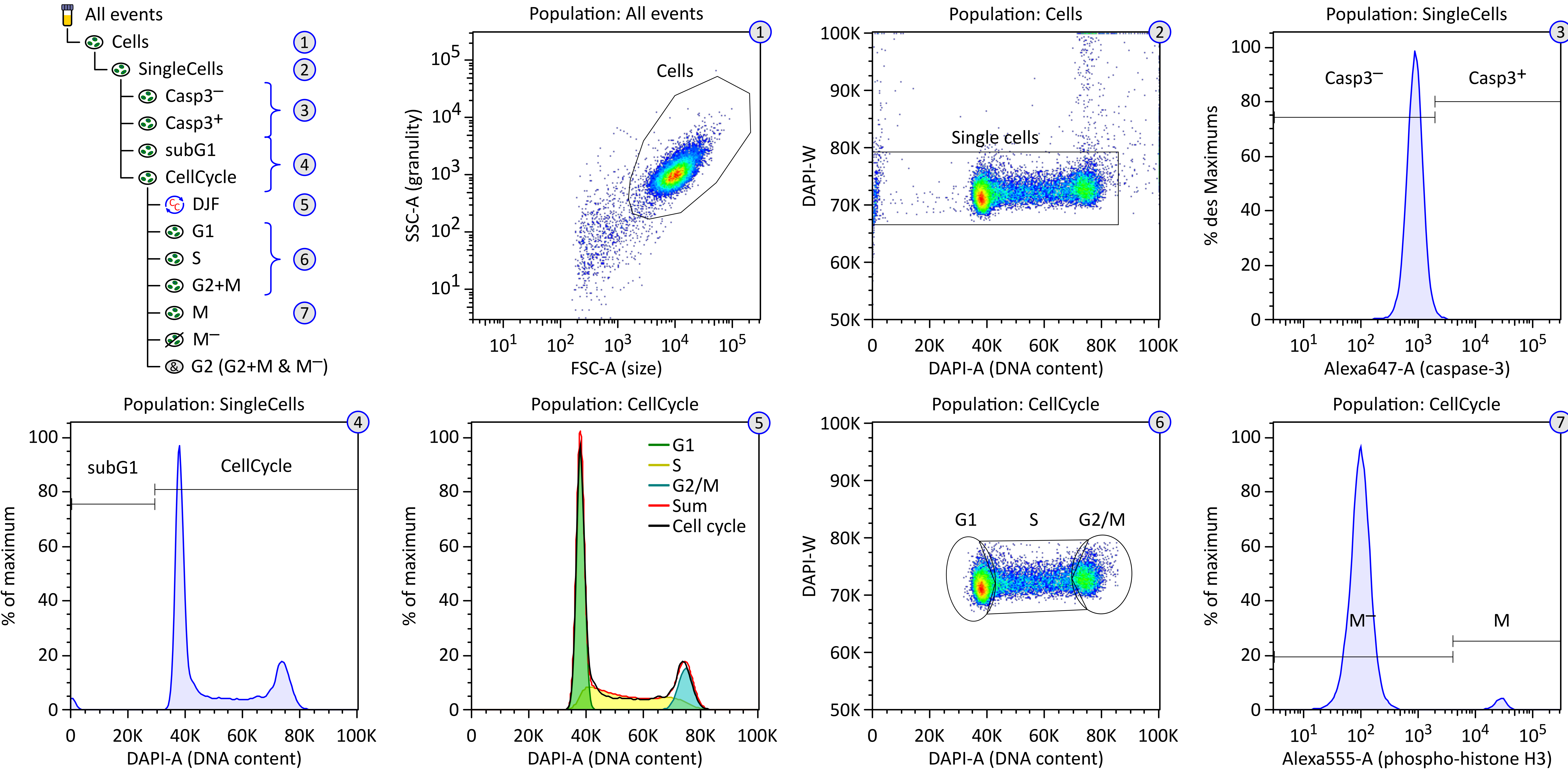




Figure 2





# Figure 3






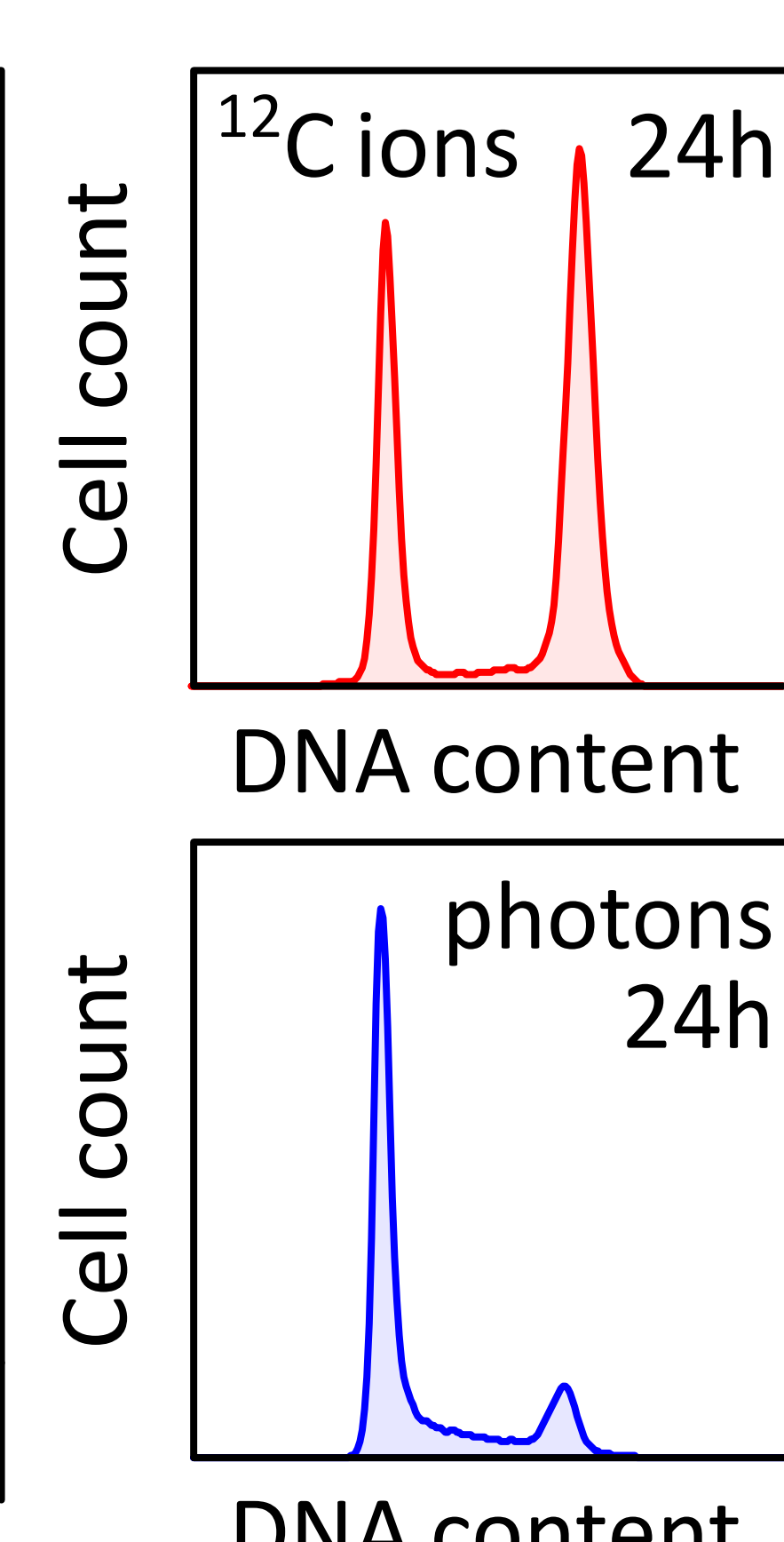
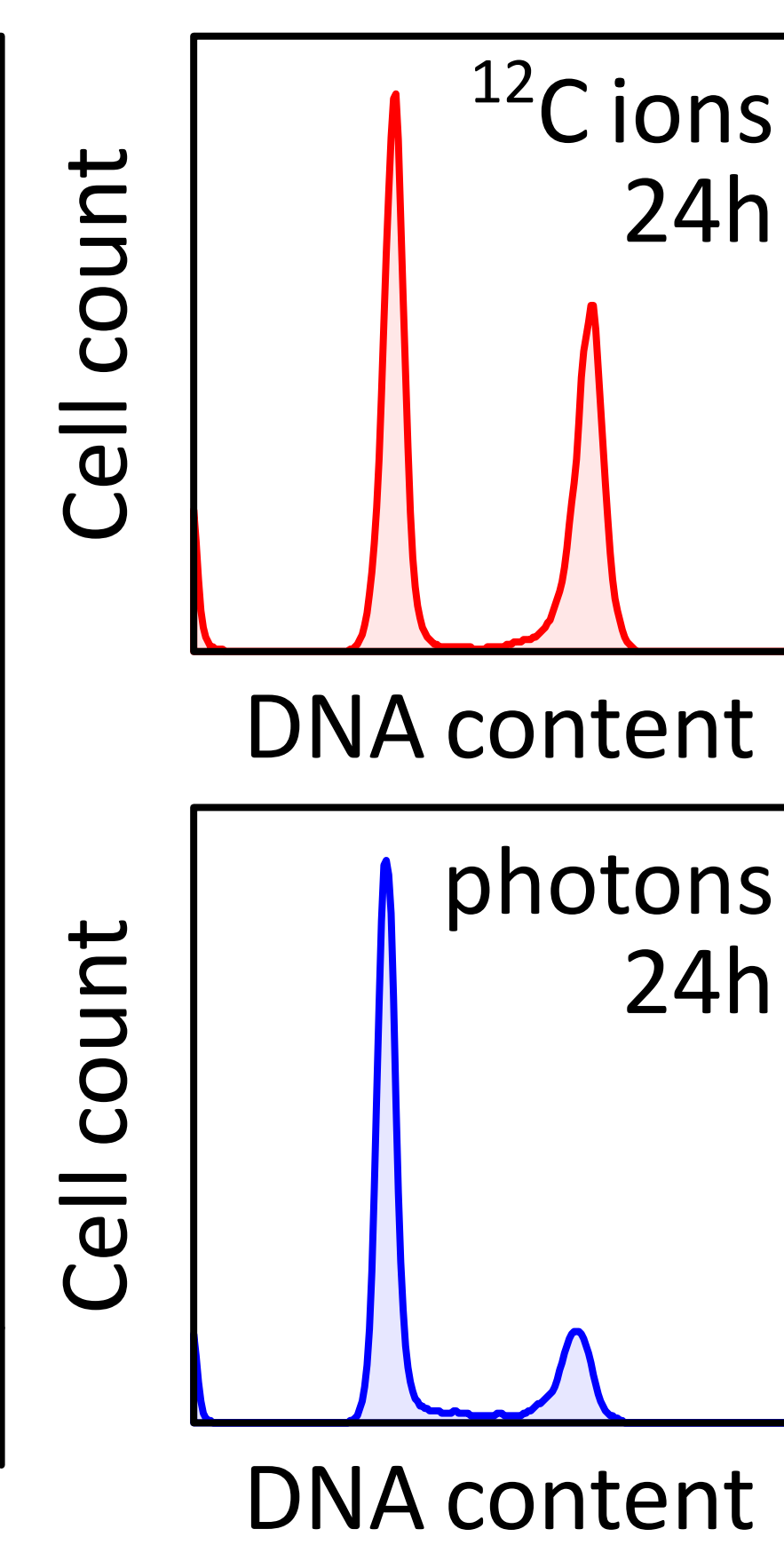
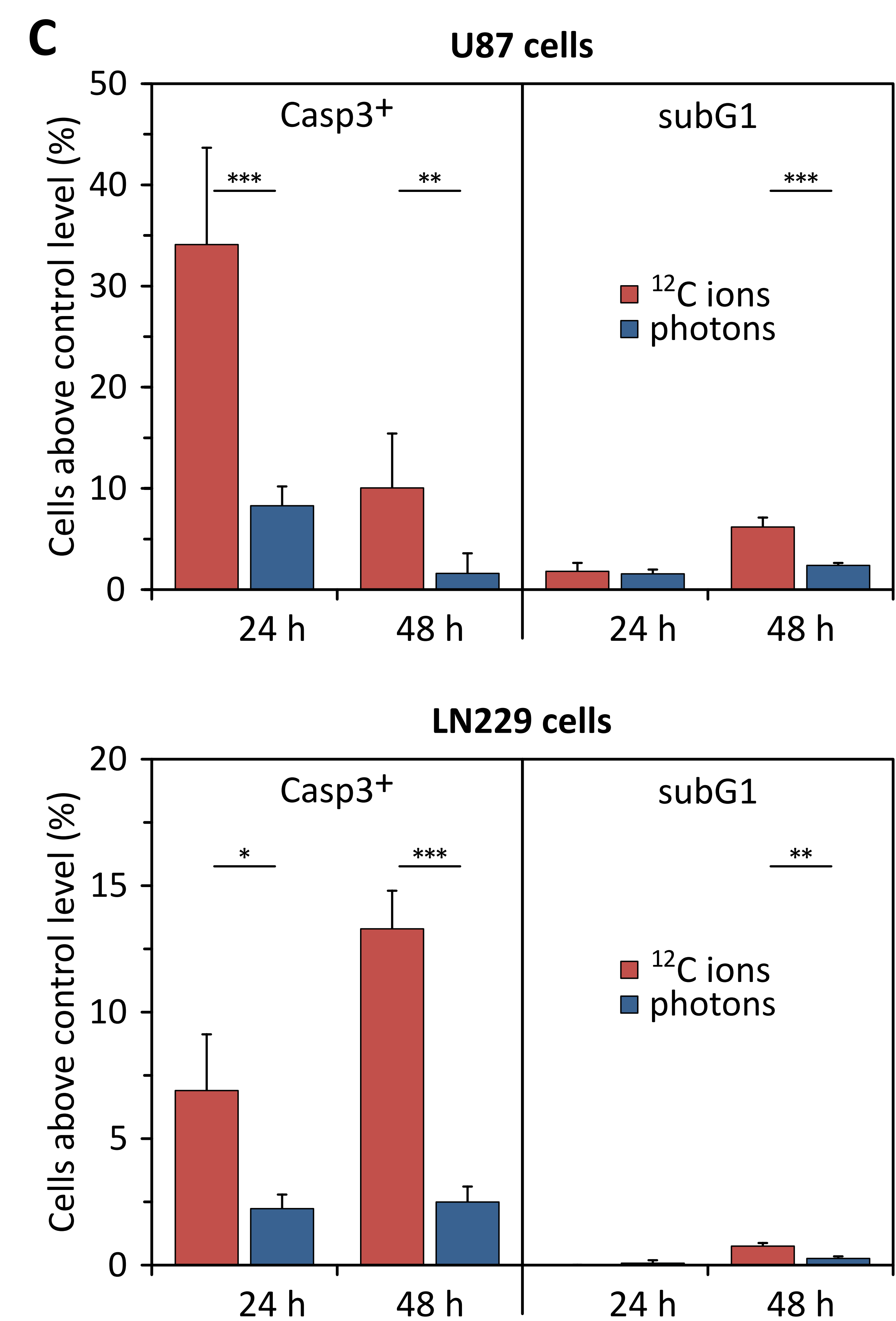
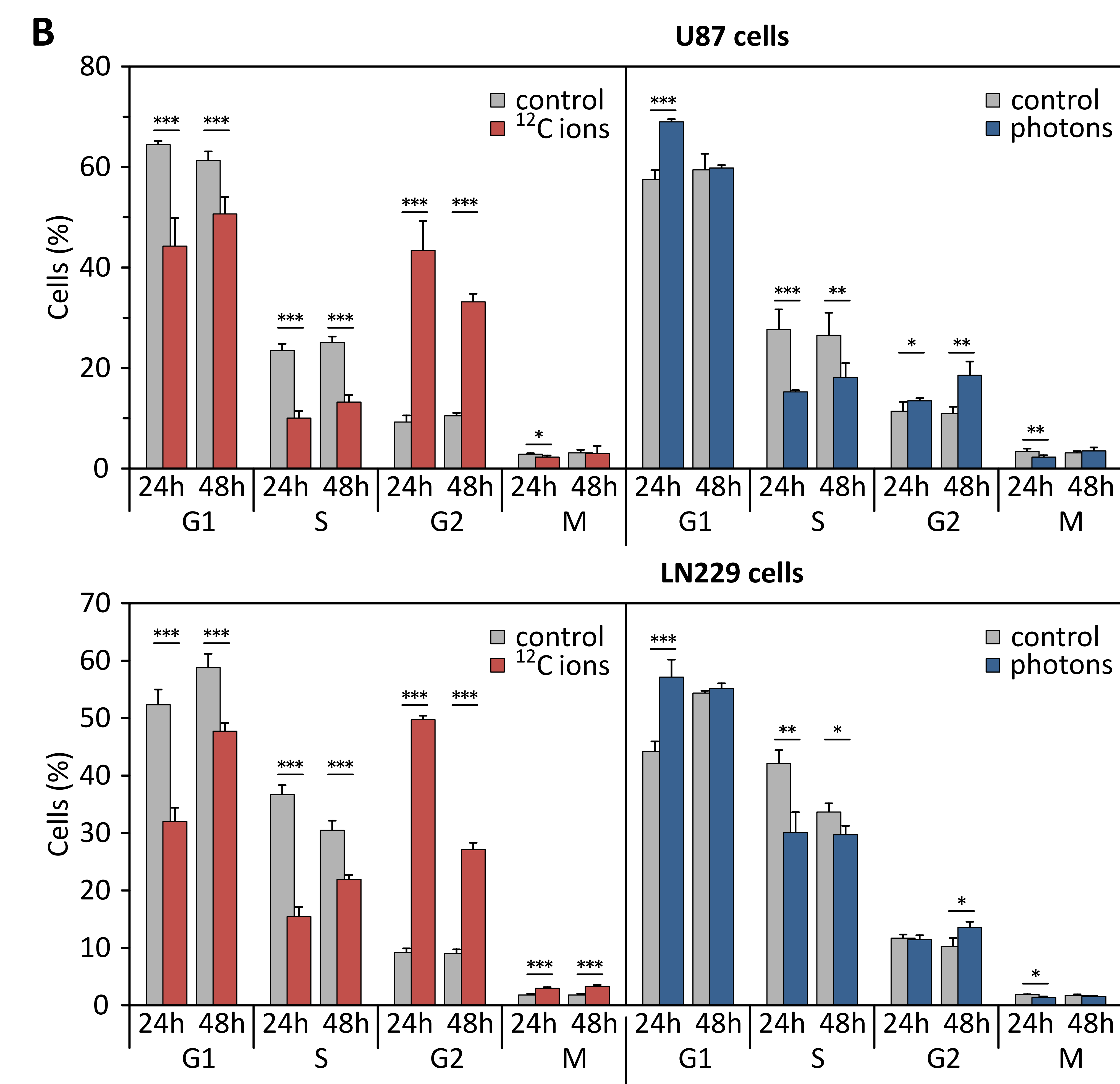
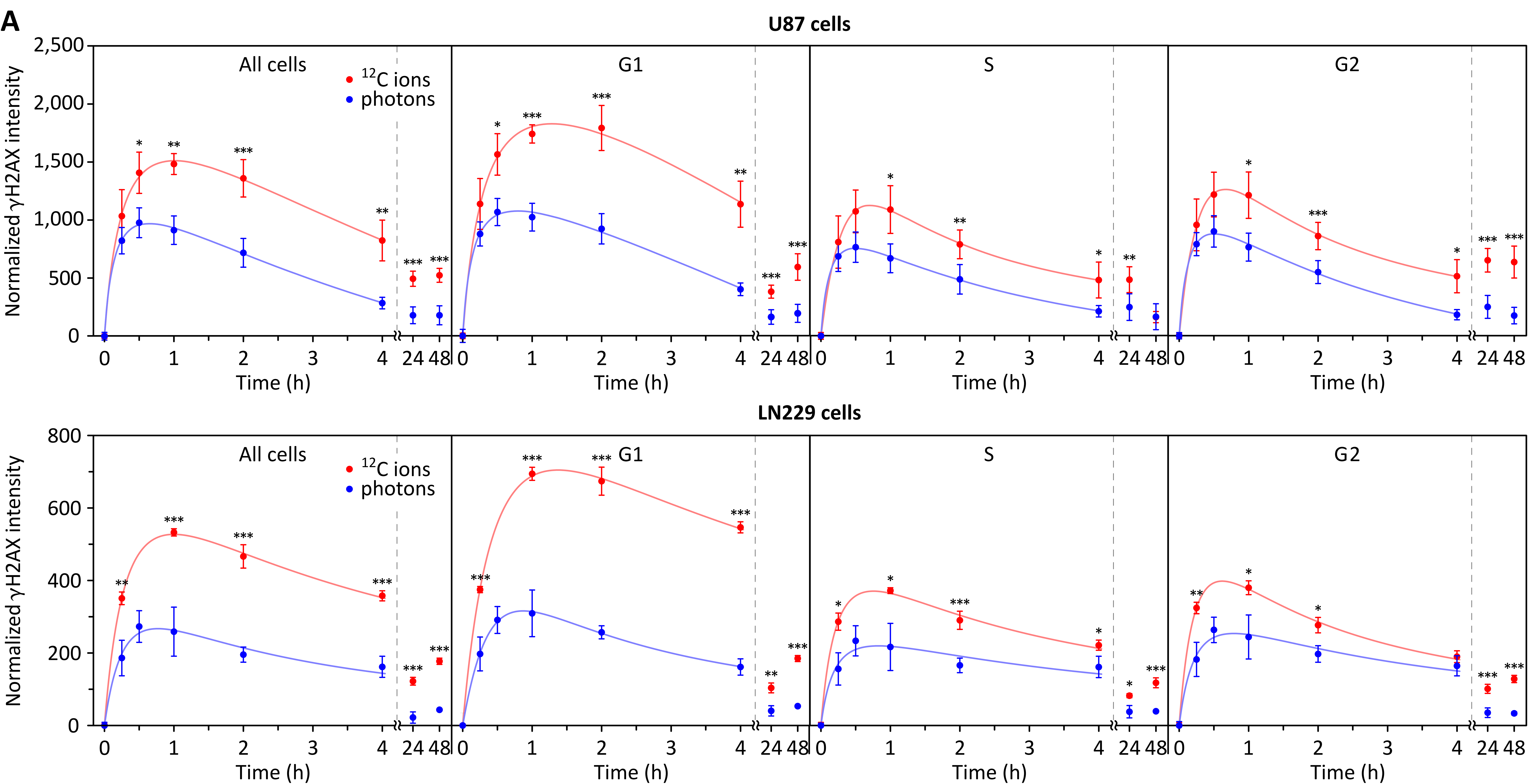
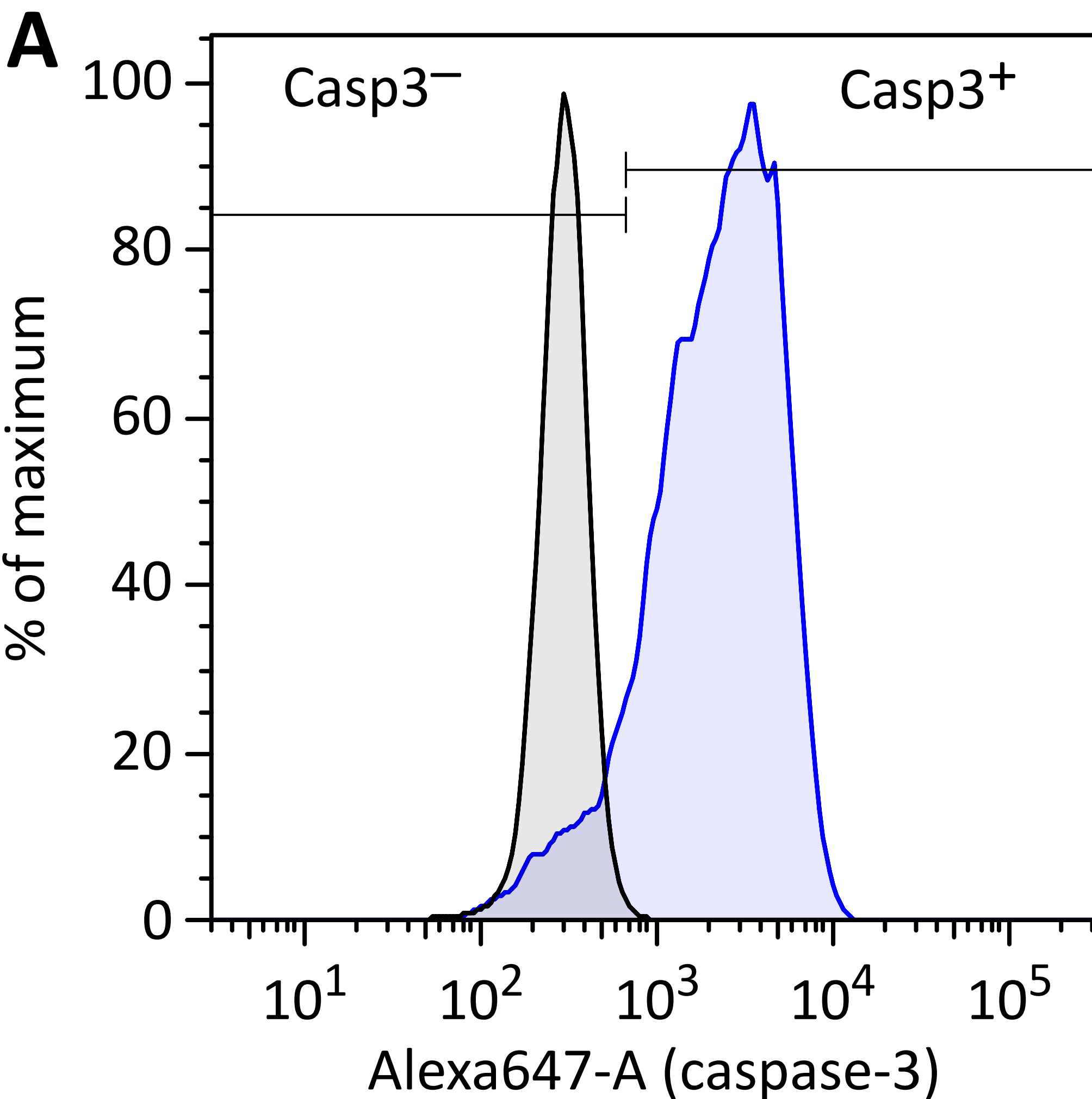
Tables: 01-May-2019.wsp					
Table Editor		Edit	Visualize		
 Tables	 Iteration	 Create Table	 To File		
			Excel Destination:  E:\Table Output		
Column	Population	Statistic	Parameter	Name	
1 $\Sigma$	Cells/SingleCells/subG1	Freq. of Parent		subG1	
2 $\Sigma$	Cells/SingleCells/CellCycle/G1	Freq. of Parent		G1	
3 $\Sigma$	Cells/SingleCells/CellCycle/S	Freq. of Parent		S	
4 $\Sigma$	Cells/SingleCells/CellCycle/G2 (G2+M...	Freq. of Parent		G2	
5 $\Sigma$	Cells/SingleCells/CellCycle/M	Freq. of Parent		M	
6 $\Sigma$	Cells/SingleCells/CellCycle/Cell Cycle	%G1		G1_DJF	
7 $\Sigma$	Cells/SingleCells/CellCycle/Cell Cycle	%S		S_DJF	
8 $\Sigma$	Cells/SingleCells/CellCycle/Cell Cycle	%G2		G2/M_DJF	
9 $\Sigma$	Cells/SingleCells/Casp3+	Freq. of Parent		Casp3+	
10 $\Sigma$	Cells/SingleCells/CellCycle	Median	Alexa488-A	gH2AX_total	
11 $\Sigma$	Cells/SingleCells/CellCycle/G1	Median	Alexa488-A	gH2AX_G1	
12 $\Sigma$	Cells/SingleCells/CellCycle/S	Median	Alexa488-A	gH2AX_S	
13 $\Sigma$	Cells/SingleCells/CellCycle/G2 (G2+M...	Median	Alexa488-A	gH2AX_G2	
14 $\Sigma$	Cells/SingleCells/CellCycle/M	Median	Alexa488-A	gH2AX_M	

Figure 4

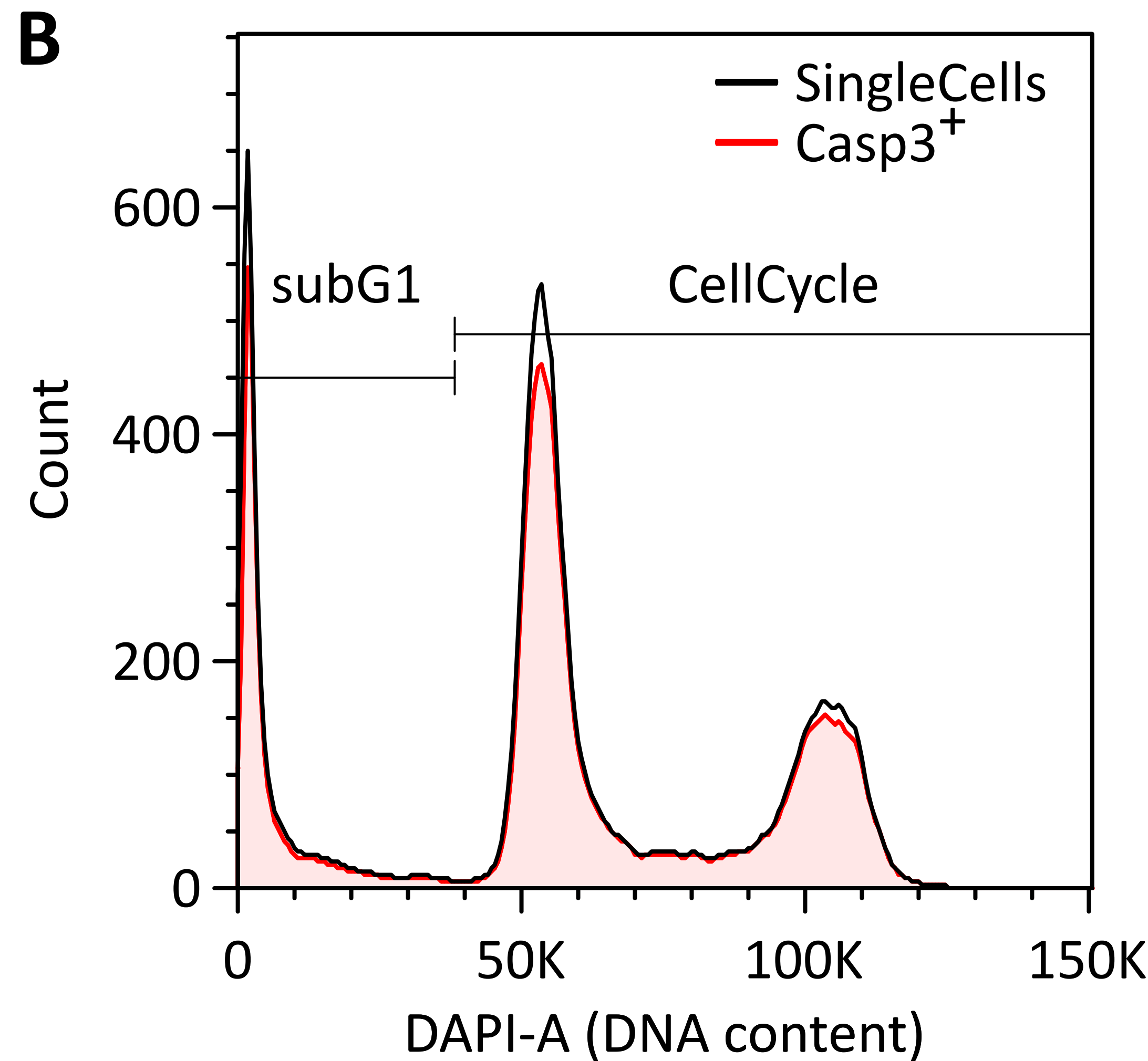




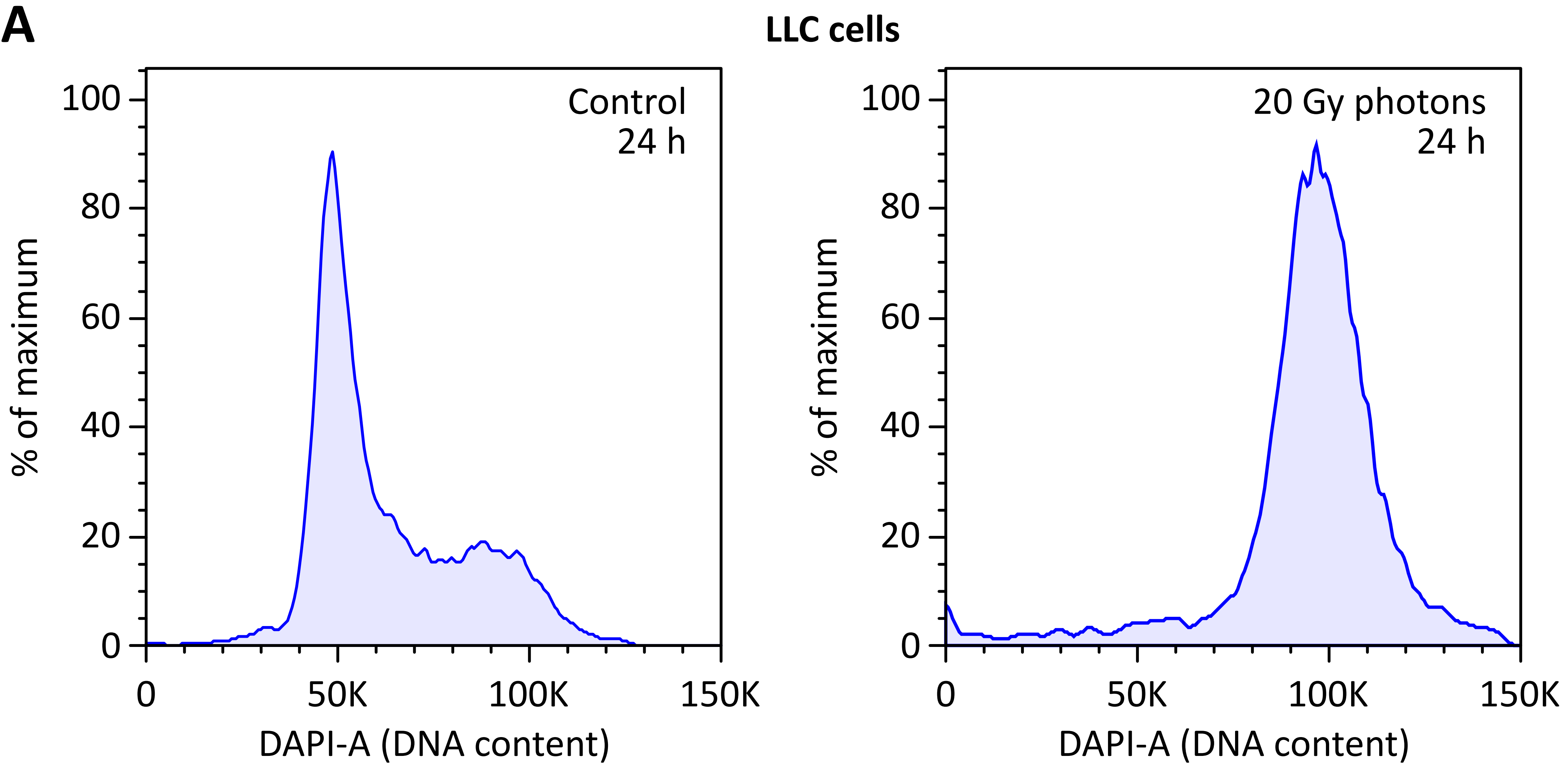
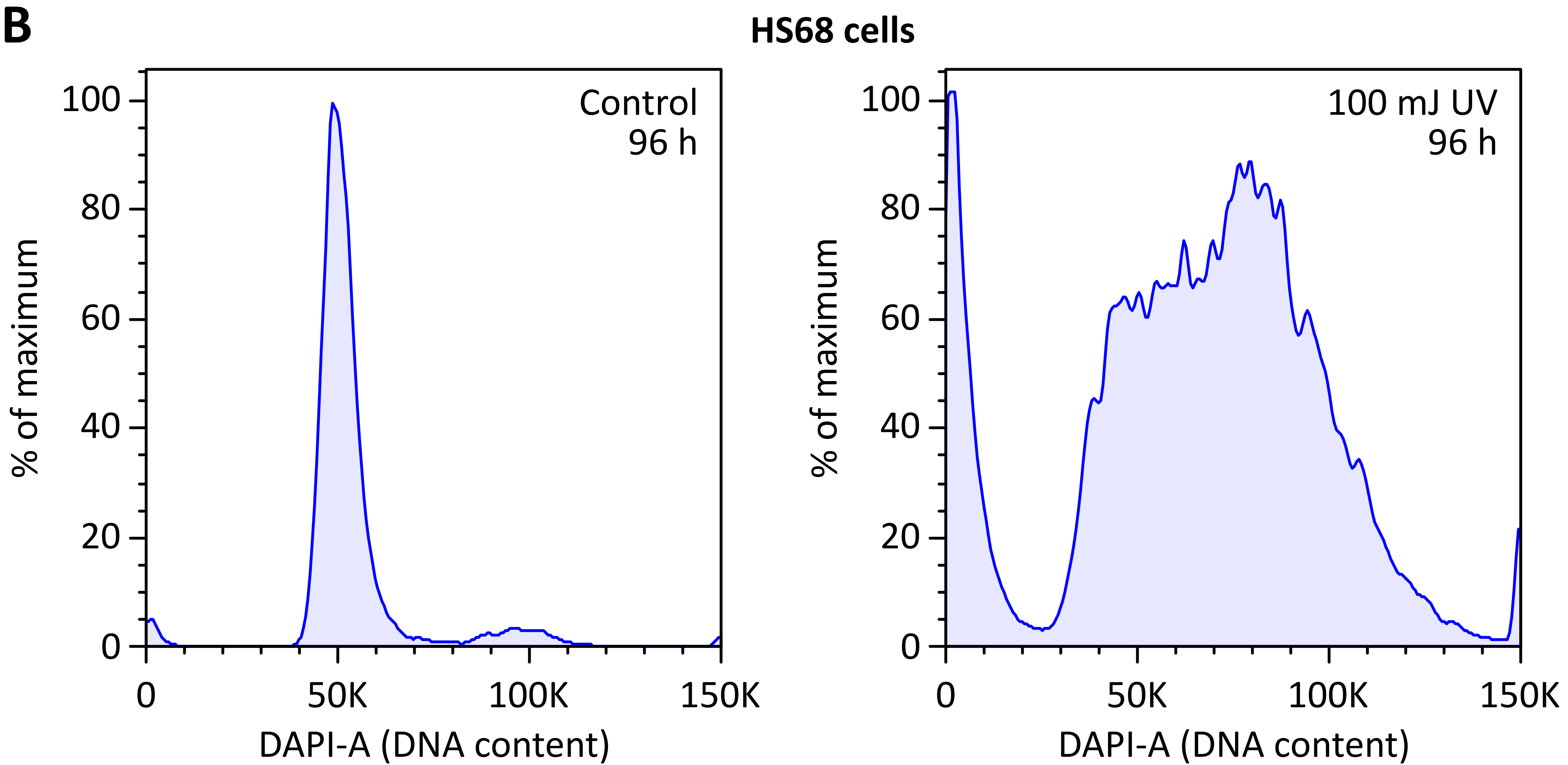
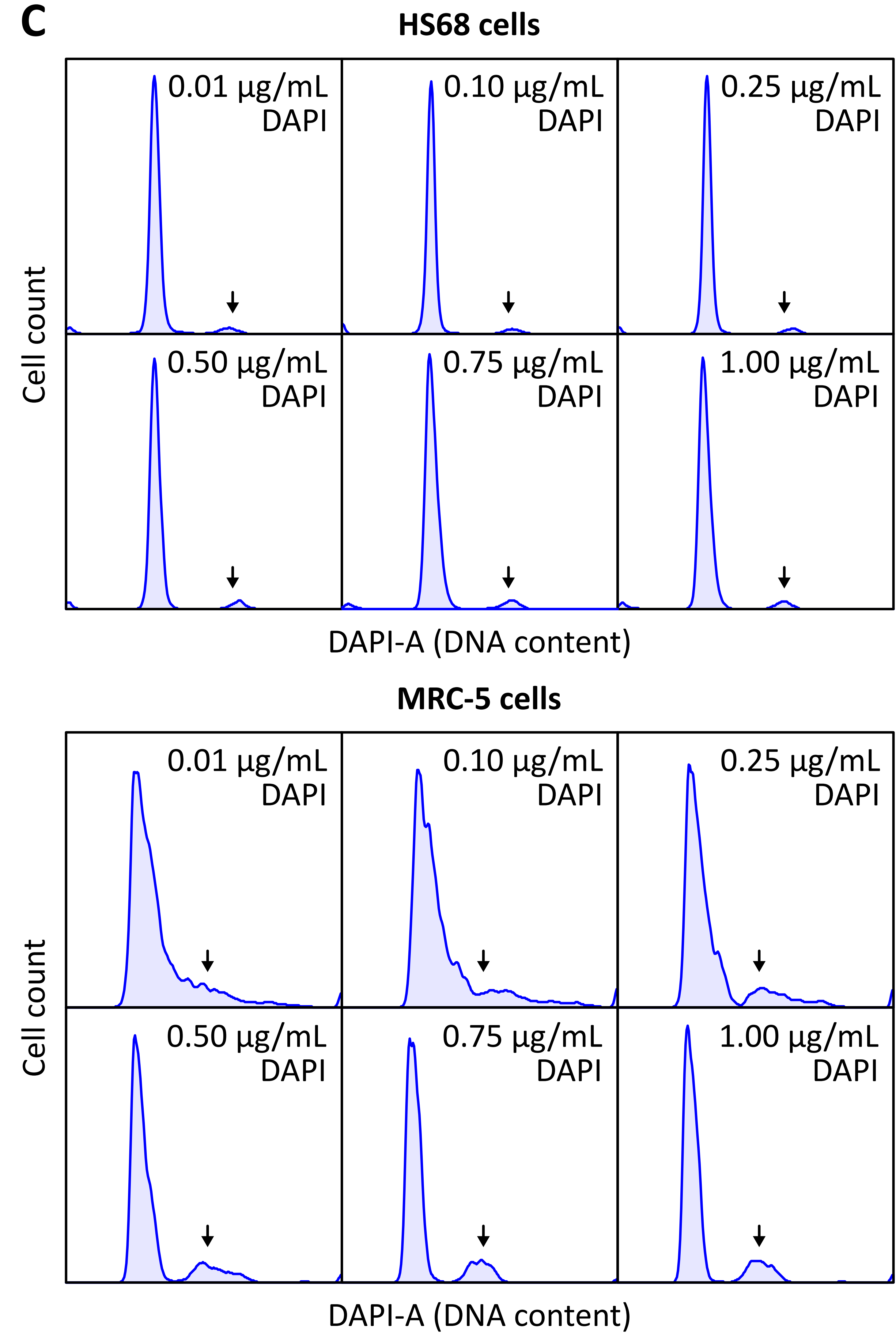
# Figure 5



Sample	% Caspase-3 <sup>+</sup>
— Control	0,7
— SuperKillerTRAIL + MG132	89,4



Population	% of parent
subG1	25.0
Casp3 <sup>+</sup>	89.4
Casp3 <sup>+</sup> & CellCycle	68.9
Casp3+ & subG1	20.5

**Figure 6****A****B****C**

Parameter	Significance	Excitation laser		Detector		Signal			
		$\lambda$ (nm)	P (mW)	Filter	U (V)	log	-A	-H	-W
FSC	front scatter (size)	488	100	488/10	50		•	•	
SSC	side scatter (granularity)	488	100	488/10	50		•	•	
Alexa488	$\gamma$ H2AX (double-strand breaks)	488	100	525/50	420	•	•	•	
Alexa555	phospho-histone H3 (M phase)	561	150	586/15	420	•	•	•	
Alexa647	active caspase-3 (apoptosis)	640	40	670/14	480	•	•	•	
DAPI	DNA (cell cycle, apoptosis)	350	20	450/50	350		•	•	•



Name of Material/ Equipment	Company
1000 µL filter tips	Nerbe plus
100-1000 µL pipette	Eppendorf
12 x 75 mm Tubes with Cell Strainer Cap, 35 µm mesh pore size	BD Falcon
15 mL tubes	BD Falcon
200 µL filter tips	Nerbe plus
20-200 µL pipette	Eppendorf
4',6-Diamidin-2-phenylindol (DAPI)	Sigma-Aldrich
Alexa Fluor 488 anti-H2A.X Phospho (Ser139) Antibody RRID: AB_2248011	BioLegend
Alexa Fluor 647 Rabbit Anti-Active Caspase-3 Antibody RRID: AB_1727414	BD Pharmingen
BD FACSClean solution	BD Biosciences
BD FACSRinse solution	BD Biosciences
Dulbecco's Phosphate Buffered Saline (PBS)	Biochrom
Dulbecco's Modified Eagle's Medium with stable glutamin	Biochrom
Ethanol absolute	VWR
Excel software	Microsoft
FBS Superior (fetal bovine serum)	Biochrom
FlowJo v10 software	LLC
Fluoromount-G	SouthernBiotech
folded cellulose filters, grade 3hw	NeoLab

LSRII or LSRFortessa cytometer	BD Biosciences
MG132	Calbiochem
Multifuge 3SR+	Heraeus
Paraformaldehyde	AppliChem
Phospho-Histone H3 (Ser10) (D2C8) XP Rabbit mAb (Alexa Fluor® 555 Conjugate) RRID: AB_10694639	Cell Signaling Technology
PIPETBOY acu 2	Integra Biosciences
Serological pipettes, 10 mL	Corning
Serological pipettes, 25 mL	Corning
Serological pipettes, 5 mL	Corning
SuperKillerTRAIL (modified TNF-related apoptosis-inducing ligand)	Biomol
T25 cell culture flasks	Greiner bio-one
Trypsin/EDTA	PAN Biotech
U87 MG glioblastoma cells	ATCC

## Catalog Number

07-693-8300

3123000063

352235

352096

07-662-8300

3123000055

D9542

613406

560626

340345

340346

L 182

FG 0415

20821.330

S 0615

online order

0100-01

11416

474787

A3813

#3475

155 016

4488

4489

4487

AG-40T-0002-C020

690160

P10-025500

ATCC-HTB-14

## Comments/Description

Dissolve in water at 200 µg/ml and store aliquots at -20 °C

Dilute 1:20

Dilute 1:20

For cytometer cleaning routine after measurement

For cytometer cleaning routine after measurement

Dissolve in water to 1x concentration

Routine cell culture material for the example cell line used  
in the protocol

Routine cell culture material for the example cell line used  
in the protocol

Embedding medium for optional preparation of microscopic  
slides from stained samples

optional drug for apoptosis positive control

Prepare 4.5% solution fresh. Dilute in PBS by heating to 80 °C with slow stirring under the fume hood. Cover the flask  
Dilute 3:200

optional drug for apoptosis positive control

Routine cell culture material for the example cell line used  
in the protocol

Routine cell culture material for the example cell line used  
in the protocol

Example cell line used in the protocol



1 Alewife Center #200  
Cambridge, MA 02140  
tel. 617.945.9051  
www.jove.com

## ARTICLE AND VIDEO LICENSE AGREEMENT

Title of Article:

Cell cycle-specific measurement of the DNA damage response after genotoxic stress by flow cytometry

Author(s):

Ramon Lopez Perez, Franziska Münz, Jonas Kröschke, Jannek Brauer, Nils H. Nicolay, Peter E. Huber

Item 1: The Author elects to have the Materials be made available (as described at <http://www.jove.com/publish>) via:

☒ Standard Access

☐ Open Access

Item 2: Please select one of the following items:

☒ The Author is **NOT** a United States government employee.

☐ The Author is a United States government employee and the Materials were prepared in the course of his or her duties as a United States government employee.

☐ The Author is a United States government employee but the Materials were NOT prepared in the course of his or her duties as a United States government employee.

### ARTICLE AND VIDEO LICENSE AGREEMENT

1. **Defined Terms.** As used in this Article and Video License Agreement, the following terms shall have the following meanings: **"Agreement"** means this Article and Video License Agreement; **"Article"** means the article specified on the last page of this Agreement, including any associated materials such as texts, figures, tables, artwork, abstracts, or summaries contained therein; **"Author"** means the author who is a signatory to this Agreement; **"Collective Work"** means a work, such as a periodical issue, anthology or encyclopedia, in which the Materials in their entirety in unmodified form, along with a number of other contributions, constituting separate and independent works in themselves, are assembled into a collective whole; **"CRC License"** means the Creative Commons Attribution-Non Commercial-No Derivs 3.0 Unported Agreement, the terms and conditions of which can be found at: <http://creativecommons.org/licenses/by-nc-nd/3.0/legalcode>; **"Derivative Work"** means a work based upon the Materials or upon the Materials and other pre-existing works, such as a translation, musical arrangement, dramatization, fictionalization, motion picture version, sound recording, art reproduction, abridgment, condensation, or any other form in which the Materials may be recast, transformed, or adapted; **"Institution"** means the institution, listed on the last page of this Agreement, by which the Author was employed at the time of the creation of the Materials; **"JoVE"** means MyJoVE Corporation, a Massachusetts corporation and the publisher of The Journal of Visualized Experiments; **"Materials"** means the Article and / or the Video; **"Parties"** means the Author and JoVE; **"Video"** means any video(s) made by the Author, alone or in conjunction with any other parties, or by JoVE or its affiliates or agents, individually or in collaboration with the Author or any other parties, incorporating all or any portion

of the Article, and in which the Author may or may not appear.

2. **Background.** The Author, who is the author of the Article, in order to ensure the dissemination and protection of the Article, desires to have the JoVE publish the Article and create and transmit videos based on the Article. In furtherance of such goals, the Parties desire to memorialize in this Agreement the respective rights of each Party in and to the Article and the Video.

3. **Grant of Rights in Article.** In consideration of JoVE agreeing to publish the Article, the Author hereby grants to JoVE, subject to **Sections 4** and **7** below, the exclusive, royalty-free, perpetual (for the full term of copyright in the Article, including any extensions thereto) license (a) to publish, reproduce, distribute, display and store the Article in all forms, formats and media whether now known or hereafter developed (including without limitation in print, digital and electronic form) throughout the world, (b) to translate the Article into other languages, create adaptations, summaries or extracts of the Article or other Derivative Works (including, without limitation, the Video) or Collective Works based on all or any portion of the Article and exercise all of the rights set forth in (a) above in such translations, adaptations, summaries, extracts, Derivative Works or Collective Works and (c) to license others to do any or all of the above. The foregoing rights may be exercised in all media and formats, whether now known or hereafter devised, and include the right to make such modifications as are technically necessary to exercise the rights in other media and formats. If the "Open Access" box has been checked in **Item 1** above, JoVE and the Author hereby grant to the public all such rights in the Article as provided in, but subject to all limitations and requirements set forth in, the CRC License.

## ARTICLE AND VIDEO LICENSE AGREEMENT

4. **Retention of Rights in Article.** Notwithstanding the exclusive license granted to JoVE in **Section 3** above, the Author shall, with respect to the Article, retain the non-exclusive right to use all or part of the Article for the non-commercial purpose of giving lectures, presentations or teaching classes, and to post a copy of the Article on the Institution's website or the Author's personal website, in each case provided that a link to the Article on the JoVE website is provided and notice of JoVE's copyright in the Article is included. All non-copyright intellectual property rights in and to the Article, such as patent rights, shall remain with the Author.

5. **Grant of Rights in Video – Standard Access.** This **Section 5** applies if the "Standard Access" box has been checked in **Item 1** above or if no box has been checked in **Item 1** above. In consideration of JoVE agreeing to produce, display or otherwise assist with the Video, the Author hereby acknowledges and agrees that, Subject to **Section 7** below, JoVE is and shall be the sole and exclusive owner of all rights of any nature, including, without limitation, all copyrights, in and to the Video. To the extent that, by law, the Author is deemed, now or at any time in the future, to have any rights of any nature in or to the Video, the Author hereby disclaims all such rights and transfers all such rights to JoVE.

6. **Grant of Rights in Video – Open Access.** This **Section 6** applies only if the "Open Access" box has been checked in **Item 1** above. In consideration of JoVE agreeing to produce, display or otherwise assist with the Video, the Author hereby grants to JoVE, subject to **Section 7** below, the exclusive, royalty-free, perpetual (for the full term of copyright in the Article, including any extensions thereto) license (a) to publish, reproduce, distribute, display and store the Video in all forms, formats and media whether now known or hereafter developed (including without limitation in print, digital and electronic form) throughout the world, (b) to translate the Video into other languages, create adaptations, summaries or extracts of the Video or other Derivative Works or Collective Works based on all or any portion of the Video and exercise all of the rights set forth in (a) above in such translations, adaptations, summaries, extracts, Derivative Works or Collective Works and (c) to license others to do any or all of the above. The foregoing rights may be exercised in all media and formats, whether now known or hereafter devised, and include the right to make such modifications as are technically necessary to exercise the rights in other media and formats. For any Video to which this **Section 6** is applicable, JoVE and the Author hereby grant to the public all such rights in the Video as provided in, but subject to all limitations and requirements set forth in, the CRC License.

7. **Government Employees.** If the Author is a United States government employee and the Article was prepared in the course of his or her duties as a United States government employee, as indicated in **Item 2** above, and any of the licenses or grants granted by the Author hereunder exceed the scope of the 17 U.S.C. 403, then the rights granted hereunder shall be limited to the maximum

rights permitted under such statute. In such case, all provisions contained herein that are not in conflict with such statute shall remain in full force and effect, and all provisions contained herein that do so conflict shall be deemed to be amended so as to provide to JoVE the maximum rights permissible within such statute.

8. **Protection of the Work.** The Author(s) authorize JoVE to take steps in the Author(s) name and on their behalf if JoVE believes some third party could be infringing or might infringe the copyright of either the Author's Article and/or Video.

9. **Likeness, Privacy, Personality.** The Author hereby grants JoVE the right to use the Author's name, voice, likeness, picture, photograph, image, biography and performance in any way, commercial or otherwise, in connection with the Materials and the sale, promotion and distribution thereof. The Author hereby waives any and all rights he or she may have, relating to his or her appearance in the Video or otherwise relating to the Materials, under all applicable privacy, likeness, personality or similar laws.

10. **Author Warranties.** The Author represents and warrants that the Article is original, that it has not been published, that the copyright interest is owned by the Author (or, if more than one author is listed at the beginning of this Agreement, by such authors collectively) and has not been assigned, licensed, or otherwise transferred to any other party. The Author represents and warrants that the author(s) listed at the top of this Agreement are the only authors of the Materials. If more than one author is listed at the top of this Agreement and if any such author has not entered into a separate Article and Video License Agreement with JoVE relating to the Materials, the Author represents and warrants that the Author has been authorized by each of the other such authors to execute this Agreement on his or her behalf and to bind him or her with respect to the terms of this Agreement as if each of them had been a party hereto as an Author. The Author warrants that the use, reproduction, distribution, public or private performance or display, and/or modification of all or any portion of the Materials does not and will not violate, infringe and/or misappropriate the patent, trademark, intellectual property or other rights of any third party. The Author represents and warrants that it has and will continue to comply with all government, institutional and other regulations, including, without limitation all institutional, laboratory, hospital, ethical, human and animal treatment, privacy, and all other rules, regulations, laws, procedures or guidelines, applicable to the Materials, and that all research involving human and animal subjects has been approved by the Author's relevant institutional review board.

11. **JoVE Discretion.** If the Author requests the assistance of JoVE in producing the Video in the Author's facility, the Author shall ensure that the presence of JoVE employees, agents or independent contractors is in accordance with the relevant regulations of the Author's institution. If more than one author is listed at the beginning of this Agreement, JoVE may, in its sole



## ARTICLE AND VIDEO LICENSE AGREEMENT

discretion, elect not take any action with respect to the Article until such time as it has received complete, executed Article and Video License Agreements from each such author. JoVE reserves the right, in its absolute and sole discretion and without giving any reason therefore, to accept or decline any work submitted to JoVE. JoVE and its employees, agents and independent contractors shall have full, unfettered access to the facilities of the Author or of the Author's institution as necessary to make the Video, whether actually published or not. JoVE has sole discretion as to the method of making and publishing the Materials, including, without limitation, to all decisions regarding editing, lighting, filming, timing of publication, if any, length, quality, content and the like.

12. **Indemnification.** The Author agrees to indemnify JoVE and/or its successors and assigns from and against any and all claims, costs, and expenses, including attorney's fees, arising out of any breach of any warranty or other representations contained herein. The Author further agrees to indemnify and hold harmless JoVE from and against any and all claims, costs, and expenses, including attorney's fees, resulting from the breach by the Author of any representation or warranty contained herein or from allegations or instances of violation of intellectual property rights, damage to the Author's or the Author's institution's facilities, fraud, libel, defamation, research, equipment, experiments, property damage, personal injury, violations of institutional, laboratory, hospital, ethical, human and animal treatment, privacy or other rules, regulations, laws, procedures or guidelines, liabilities and other losses or damages related in any way to the submission of work to JoVE, making of videos by JoVE, or publication in JoVE or elsewhere by JoVE. The Author shall be responsible for, and shall hold JoVE harmless from, damages caused by lack of sterilization, lack of cleanliness or by contamination due to

the making of a video by JoVE its employees, agents or independent contractors. All sterilization, cleanliness or decontamination procedures shall be solely the responsibility of the Author and shall be undertaken at the Author's expense. All indemnifications provided herein shall include JoVE's attorney's fees and costs related to said losses or damages. Such indemnification and holding harmless shall include such losses or damages incurred by, or in connection with, acts or omissions of JoVE, its employees, agents or independent contractors.

13. **Fees.** To cover the cost incurred for publication, JoVE must receive payment before production and publication the Materials. Payment is due in 21 days of invoice. Should the Materials not be published due to an editorial or production decision, these funds will be returned to the Author. Withdrawal by the Author of any submitted Materials after final peer review approval will result in a US\$1,200 fee to cover pre-production expenses incurred by JoVE. If payment is not received by the completion of filming, production and publication of the Materials will be suspended until payment is received.

14. **Transfer, Governing Law.** This Agreement may be assigned by JoVE and shall inure to the benefits of any of JoVE's successors and assignees. This Agreement shall be governed and construed by the internal laws of the Commonwealth of Massachusetts without giving effect to any conflict of law provision thereunder. This Agreement may be executed in counterparts, each of which shall be deemed an original, but all of which together shall be deemed to be one and the same agreement. A signed copy of this Agreement delivered by facsimile, e-mail or other means of electronic transmission shall be deemed to have the same legal effect as delivery of an original signed copy of this Agreement.

A signed copy of this document must be sent with all new submissions. Only one Agreement is required per submission.

### CORRESPONDING AUTHOR

Name:

Ramon Lopez Perez

Department:

Molecular and Radiation Oncology


Institution:

German Cancer Research Center

Title:

Dr. rer. nat. (PhD)

Signature:



Date:

March 5, 2019

Please submit a **signed and dated** copy of this license by one of the following three methods:

1. Upload an electronic version on the JoVE submission site
2. Fax the document to +1.866.381.2236
3. Mail the document to JoVE / Attn: JoVE Editorial / 1 Alewife Center #200 / Cambridge, MA 02140

## Responses to the reviewer comments

### Reviewer #1:

#### Manuscript Summary:

The reviewed manuscript will be very helpful for all users of flow cytometry. The authors describe protocol for cell cycle-specific measurement of the DNA damage response after genotoxic stress by flow cytometry. They propose the solution for measure during one experiment of all stages of the DNA damage response, cell cycle and cell death by apoptosis in a case of repair failure. The all procedures are described in details.

So, I recommend this manuscript to publication in JoVE without any revision.

[Thank you for reviewing our manuscript and for the positive comments.](#)

### Reviewer #2:

#### Manuscript Summary:

Authors describe a useful method for determining, at the same time,  $\gamma$ H2AX, caspase-3, subG1 and cell cycle distribution. They present some experiments with U87 and LN229 cells treated with radiation.

Overall, the method is useful also for other applications upon appropriate adaptation.

[Thank you for reviewing our manuscript.](#)

#### Major Concerns:

There is only one caveat. The title and terminology throughout the manuscript suggests that the DNA damage response (DDR) has been measured. DDR is complex involving apical and downstream kinases such as ATM/ATR/DNA-PK, CHK1, CHK2, and a plethora of targets of ATM/ATR. In this manuscript, only  $\gamma$ H2AX is determined as a specific outread of DDR, while caspase-3 and subG1 can also be induced by non-genotoxic exposures (e.g. TRAIL activation). Thus, the title is somewhat misleading and should be changed to what is actually demonstrated here: Cell cycle specific measurement of  $\gamma$ H2AX and apoptosis after genotoxic stress by flow cytometry.

[We thank the reviewer for the clarifications. We do agree that our method only covers some specific aspects of the DDR, albeit important ones from all stages of the DDR. Therefore, we have changed the title of the manuscript in the revision as suggested by the reviewer.](#)

#### Minor Concerns:

##### Specific comments:

- Line 195: specify "DNA damage response" ( $\gamma$ H2AX was measured together with...)

[The sentence was changed to "Cell cycle-specific  \$\gamma\$ H2AX levels and apoptosis were measured..."](#)

- Line 204: "higher rate of apoptosis", and line 208: "statistically significant different effects".

However, in Fig. 3C, subG1 is only slightly enhanced, in LN229 borderline (1 or 2% apoptosis). Is this significant compared to the control? What is the level in the non-treated control? Why is the yield so low?

[The differences in apoptosis induction between carbon ion and photon radiation were indeed statistically significant for caspase-3 activation, as well as subG1, at least at 48 h \(even though the statement "statistically significant different effects" is not used in that specific context, but rather for](#)

the whole dataset as an example of an optimal outcome). This was also true when looking at the raw subG1 values without subtraction of control levels (~0.5% subG1 in LN229 and ~1% in U87). In comparison to caspase-3 activation, the subG1 levels were however much lower in both cell lines. Possible reasons for this include:

- 1) DNA degradation happens downstream of caspase-3 activation and was probably not yet at its peak level at the observed time points (as also mentioned in the legend of Figure 4)
- 2) Our gating strategy ensures that only cells of normal size are evaluated; apoptotic bodies are excluded to avoid overestimation of the subG1 population (we do not know in how many bodies one cell may decompose). On the other side, we might miss some subG1 cells in this way
- 3) We have observed that the consistency between caspase-3 and subG1 levels varies a lot between different cell lines and treatments and it might well be that it also depends on the pathway choice of apoptosis or apoptosis-like processes

While some of the aspects are covered in the manuscript, a full discussion of these points would probably go beyond the scope of the results section and the methodical aspects that we wanted to focus on. Therefore, for a more in-depth-discussion we referred to our published work, which also covers the potential discrepancies between the caspase-3 and subG1 levels.

- Line 220: Fig. 5C. I cannot see much difference with increasing concentration of DAP1. Remove this statement or specify more precisely.

To make this point clearer, we have highlighted the position of the G2/M peak in the histograms with an arrow and rephrased the text to draw the attention of the reader to the poor definition of the G2/M shape and separation from G1 at DAPI concentrations below 0.75 µg/mL in MRC-5 cells.

- Line 227: I, personally, like the Neubauer chamber. But there are others, even more elegant methods, of cell number determination that others prefer to use. Therefore, add...."or by other means".

The sentence was changed as suggested in the revision.

- Line 300: Is it clear that true DSBs have been measured by flow cytometry in the high dose range or can the linear dose-response also be due to caspase-CAD-mediated DNA cleavage, which is an outread of apoptosis? Is caspase-3/7 already activated at these early time points?

It has indeed been described that γH2AX induction can occur in the course of DNA degradation during apoptosis. However, in this case a very strong pan-nuclear induction is observed instead of discrete foci. From quantitative microscopic measurements of foci and pan-nuclear intensity, we know that this was not the case in our cells and context. In addition, we have not observed caspase-3 activation at time points earlier than 24 h.

- Line 323-328: This is an interesting point raised by the authors. The paper would benefit much, if a picture of γH2AX foci was shown.

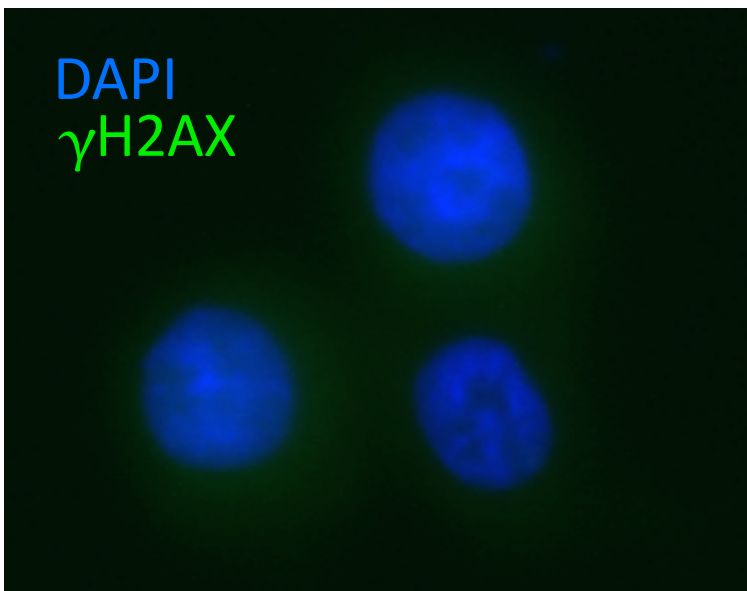
In the revision we have now included a picture of γH2AX foci prepared and acquired in the described way that also demonstrates the problem of foci overlap at high levels of DNA damage (supplementary figure 1).

- Can the method be extended with caspase-7, -9 and -8 antibodies? Please, discuss this briefly.

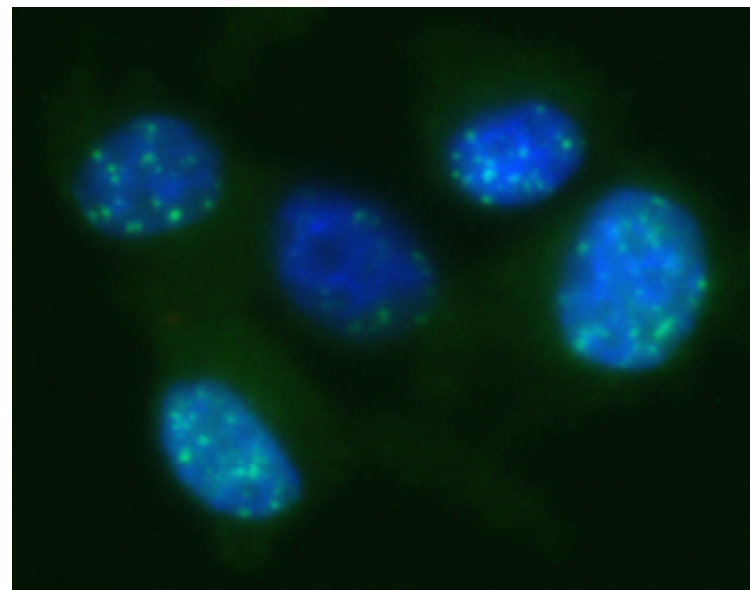
This is of course an option if apoptosis is the main process of interest. As suggested, we have included this possibility in the revised discussion.

# Supplementary Figure 1

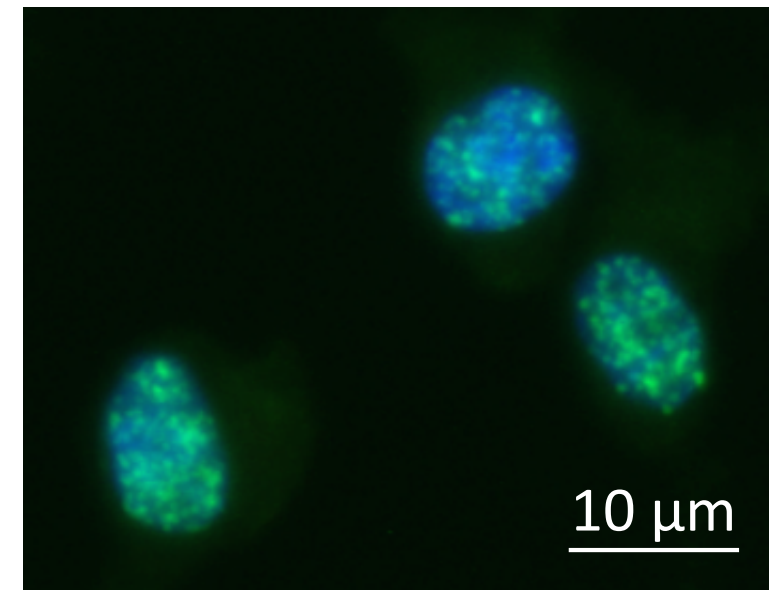
control



1 Gy



8 Gy



## ELSEVIER LICENSE TERMS AND CONDITIONS

May 06, 2019

This Agreement between German Cancer Research Center -- Ramon Lopez Perez ("You") and Elsevier ("Elsevier") consists of your license details and the terms and conditions provided by Elsevier and Copyright Clearance Center.

License Number	4583160392918
License date	May 06, 2019
Licensed Content Publisher	Elsevier
Licensed Content Publication	Radiotherapy and Oncology
Licensed Content Title	DNA damage response of clinical carbon ion versus photon radiation in human glioblastoma cells
Licensed Content Author	Ramon Lopez Perez,Nils H. Nicolay,Jörg-Christian Wolf,Moritz Frister,Peter Schmezer,Klaus-Josef Weber,Peter E. Huber
Licensed Content Date	Apr 1, 2019
Licensed Content Volume	133
Licensed Content Issue	n/a
Licensed Content Pages	10
Start Page	77
End Page	86
Type of Use	reuse in a journal/magazine
Requestor type	academic/educational institute
Intended publisher of new work	Other
Portion	figures/tables/illustrations
Number of figures/tables /illustrations	2
Format	electronic
Are you the author of this Elsevier article?	Yes
Will you be translating?	No
Order reference number	4532480545668
Original figure numbers	Figure 5a,c Supplementary Figure 2a
Title of the article	Cell cycle-specific measurement of $\gamma$ H2AX and apoptosis after genotoxic stress by flow cytometry
Publication new article is in	Journal of Visualized Experiments
Publisher of the new article	MyJove Corp.
Author of new article	Ramon Lopez Perez
Expected publication date	Sep 2019
Estimated size of new article (number of pages)	6

Requestor Location	German Cancer Research Center im Neuenheimer Feld 280  Heidelberg, 69120 Germany Attn: German Cancer Research Center
Publisher Tax ID	GB 494 6272 12
Total	0.00 EUR
Terms and Conditions	

### INTRODUCTION

1. The publisher for this copyrighted material is Elsevier. By clicking "accept" in connection with completing this licensing transaction, you agree that the following terms and conditions apply to this transaction (along with the Billing and Payment terms and conditions established by Copyright Clearance Center, Inc. ("CCC"), at the time that you opened your Rightslink account and that are available at any time at <http://myaccount.copyright.com>).

### GENERAL TERMS

2. Elsevier hereby grants you permission to reproduce the aforementioned material subject to the terms and conditions indicated.

3. Acknowledgement: If any part of the material to be used (for example, figures) has appeared in our publication with credit or acknowledgement to another source, permission must also be sought from that source. If such permission is not obtained then that material may not be included in your publication/copies. Suitable acknowledgement to the source must be made, either as a footnote or in a reference list at the end of your publication, as follows:

"Reprinted from Publication title, Vol /edition number, Author(s), Title of article / title of chapter, Pages No., Copyright (Year), with permission from Elsevier [OR APPLICABLE SOCIETY COPYRIGHT OWNER]." Also Lancet special credit - "Reprinted from The Lancet, Vol. number, Author(s), Title of article, Pages No., Copyright (Year), with permission from Elsevier."

4. Reproduction of this material is confined to the purpose and/or media for which permission is hereby given.

5. Altering/Modifying Material: Not Permitted. However figures and illustrations may be altered/adapted minimally to serve your work. Any other abbreviations, additions, deletions and/or any other alterations shall be made only with prior written authorization of Elsevier Ltd. (Please contact Elsevier at [permissions@elsevier.com](mailto:permissions@elsevier.com)). No modifications can be made to any Lancet figures/tables and they must be reproduced in full.

6. If the permission fee for the requested use of our material is waived in this instance, please be advised that your future requests for Elsevier materials may attract a fee.

7. Reservation of Rights: Publisher reserves all rights not specifically granted in the combination of (i) the license details provided by you and accepted in the course of this licensing transaction, (ii) these terms and conditions and (iii) CCC's Billing and Payment terms and conditions.

8. License Contingent Upon Payment: While you may exercise the rights licensed immediately upon issuance of the license at the end of the licensing process for the transaction, provided that you have disclosed complete and accurate details of your proposed use, no license is finally effective unless and until full payment is received from you (either by publisher or by CCC) as provided in CCC's Billing and Payment terms and conditions. If full payment is not received on a timely basis, then any license preliminarily granted shall be deemed automatically revoked and shall be void as if never granted. Further, in the event

that you breach any of these terms and conditions or any of CCC's Billing and Payment terms and conditions, the license is automatically revoked and shall be void as if never granted. Use of materials as described in a revoked license, as well as any use of the materials beyond the scope of an unrevoked license, may constitute copyright infringement and publisher reserves the right to take any and all action to protect its copyright in the materials.

9. Warranties: Publisher makes no representations or warranties with respect to the licensed material.

10. Indemnity: You hereby indemnify and agree to hold harmless publisher and CCC, and their respective officers, directors, employees and agents, from and against any and all claims arising out of your use of the licensed material other than as specifically authorized pursuant to this license.

11. No Transfer of License: This license is personal to you and may not be sublicensed, assigned, or transferred by you to any other person without publisher's written permission.

12. No Amendment Except in Writing: This license may not be amended except in a writing signed by both parties (or, in the case of publisher, by CCC on publisher's behalf).

13. Objection to Contrary Terms: Publisher hereby objects to any terms contained in any purchase order, acknowledgment, check endorsement or other writing prepared by you, which terms are inconsistent with these terms and conditions or CCC's Billing and Payment terms and conditions. These terms and conditions, together with CCC's Billing and Payment terms and conditions (which are incorporated herein), comprise the entire agreement between you and publisher (and CCC) concerning this licensing transaction. In the event of any conflict between your obligations established by these terms and conditions and those established by CCC's Billing and Payment terms and conditions, these terms and conditions shall control.

14. Revocation: Elsevier or Copyright Clearance Center may deny the permissions described in this License at their sole discretion, for any reason or no reason, with a full refund payable to you. Notice of such denial will be made using the contact information provided by you. Failure to receive such notice will not alter or invalidate the denial. In no event will Elsevier or Copyright Clearance Center be responsible or liable for any costs, expenses or damage incurred by you as a result of a denial of your permission request, other than a refund of the amount(s) paid by you to Elsevier and/or Copyright Clearance Center for denied permissions.

### LIMITED LICENSE

The following terms and conditions apply only to specific license types:

15. **Translation:** This permission is granted for non-exclusive world **English** rights only unless your license was granted for translation rights. If you licensed translation rights you may only translate this content into the languages you requested. A professional translator must perform all translations and reproduce the content word for word preserving the integrity of the article.

16. **Posting licensed content on any Website:** The following terms and conditions apply as follows: Licensing material from an Elsevier journal: All content posted to the web site must maintain the copyright information line on the bottom of each image; A hyper-text must be included to the Homepage of the journal from which you are licensing at <http://www.sciencedirect.com/science/journal/xxxxx> or the Elsevier homepage for books at <http://www.elsevier.com>; Central Storage: This license does not include permission for a scanned version of the material to be stored in a central repository such as that provided by Heron/XanEdu.

Licensing material from an Elsevier book: A hyper-text link must be included to the Elsevier homepage at <http://www.elsevier.com>. All content posted to the web site must maintain the copyright information line on the bottom of each image.



**Posting licensed content on Electronic reserve:** In addition to the above the following clauses are applicable: The web site must be password-protected and made available only to bona fide students registered on a relevant course. This permission is granted for 1 year only. You may obtain a new license for future website posting.

**17. For journal authors:** the following clauses are applicable in addition to the above:

**Preprints:**

A preprint is an author's own write-up of research results and analysis, it has not been peer-reviewed, nor has it had any other value added to it by a publisher (such as formatting, copyright, technical enhancement etc.).

Authors can share their preprints anywhere at any time. Preprints should not be added to or enhanced in any way in order to appear more like, or to substitute for, the final versions of articles however authors can update their preprints on arXiv or RePEc with their Accepted Author Manuscript (see below).

If accepted for publication, we encourage authors to link from the preprint to their formal publication via its DOI. Millions of researchers have access to the formal publications on ScienceDirect, and so links will help users to find, access, cite and use the best available version. Please note that Cell Press, The Lancet and some society-owned have different preprint policies. Information on these policies is available on the journal homepage.

**Accepted Author Manuscripts:** An accepted author manuscript is the manuscript of an article that has been accepted for publication and which typically includes author-incorporated changes suggested during submission, peer review and editor-author communications.

Authors can share their accepted author manuscript:

- immediately
  - via their non-commercial person homepage or blog
  - by updating a preprint in arXiv or RePEc with the accepted manuscript
  - via their research institute or institutional repository for internal institutional uses or as part of an invitation-only research collaboration work-group
  - directly by providing copies to their students or to research collaborators for their personal use
  - for private scholarly sharing as part of an invitation-only work group on commercial sites with which Elsevier has an agreement
- After the embargo period
  - via non-commercial hosting platforms such as their institutional repository
  - via commercial sites with which Elsevier has an agreement

In all cases accepted manuscripts should:

- link to the formal publication via its DOI
- bear a CC-BY-NC-ND license - this is easy to do
- if aggregated with other manuscripts, for example in a repository or other site, be shared in alignment with our hosting policy not be added to or enhanced in any way to appear more like, or to substitute for, the published journal article.

**Published journal article (JPA):** A published journal article (PJA) is the definitive final record of published research that appears or will appear in the journal and embodies all value-adding publishing activities including peer review co-ordination, copy-editing, formatting, (if relevant) pagination and online enrichment.

Policies for sharing publishing journal articles differ for subscription and gold open access



articles:

**Subscription Articles:** If you are an author, please share a link to your article rather than the full-text. Millions of researchers have access to the formal publications on ScienceDirect, and so links will help your users to find, access, cite, and use the best available version. Theses and dissertations which contain embedded PJAs as part of the formal submission can be posted publicly by the awarding institution with DOI links back to the formal publications on ScienceDirect.

If you are affiliated with a library that subscribes to ScienceDirect you have additional private sharing rights for others' research accessed under that agreement. This includes use for classroom teaching and internal training at the institution (including use in course packs and courseware programs), and inclusion of the article for grant funding purposes.

**Gold Open Access Articles:** May be shared according to the author-selected end-user license and should contain a [CrossMark logo](#), the end user license, and a DOI link to the formal publication on ScienceDirect.

Please refer to Elsevier's [posting policy](#) for further information.

18. **For book authors** the following clauses are applicable in addition to the above:

Authors are permitted to place a brief summary of their work online only. You are not allowed to download and post the published electronic version of your chapter, nor may you scan the printed edition to create an electronic version. **Posting to a repository:** Authors are permitted to post a summary of their chapter only in their institution's repository.

19. **Thesis/Dissertation:** If your license is for use in a thesis/dissertation your thesis may be submitted to your institution in either print or electronic form. Should your thesis be published commercially, please reapply for permission. These requirements include permission for the Library and Archives of Canada to supply single copies, on demand, of the complete thesis and include permission for Proquest/UMI to supply single copies, on demand, of the complete thesis. Should your thesis be published commercially, please reapply for permission. Theses and dissertations which contain embedded PJAs as part of the formal submission can be posted publicly by the awarding institution with DOI links back to the formal publications on ScienceDirect.

### **Elsevier Open Access Terms and Conditions**

You can publish open access with Elsevier in hundreds of open access journals or in nearly 2000 established subscription journals that support open access publishing. Permitted third party re-use of these open access articles is defined by the author's choice of Creative Commons user license. See our [open access license policy](#) for more information.

#### **Terms & Conditions applicable to all Open Access articles published with Elsevier:**

Any reuse of the article must not represent the author as endorsing the adaptation of the article nor should the article be modified in such a way as to damage the author's honour or reputation. If any changes have been made, such changes must be clearly indicated.

The author(s) must be appropriately credited and we ask that you include the end user license and a DOI link to the formal publication on ScienceDirect.

If any part of the material to be used (for example, figures) has appeared in our publication with credit or acknowledgement to another source it is the responsibility of the user to ensure their reuse complies with the terms and conditions determined by the rights holder.

#### **Additional Terms & Conditions applicable to each Creative Commons user license:**

**CC BY:** The CC-BY license allows users to copy, to create extracts, abstracts and new works from the Article, to alter and revise the Article and to make commercial use of the Article (including reuse and/or resale of the Article by commercial entities), provided the user gives appropriate credit (with a link to the formal publication through the relevant DOI), provides a link to the license, indicates if changes were made and the licensor is not represented as endorsing the use made of the work. The full details of the license are

available at <http://creativecommons.org/licenses/by/4.0>.

**CC BY NC SA:** The CC BY-NC-SA license allows users to copy, to create extracts, abstracts and new works from the Article, to alter and revise the Article, provided this is not done for commercial purposes, and that the user gives appropriate credit (with a link to the formal publication through the relevant DOI), provides a link to the license, indicates if changes were made and the licensor is not represented as endorsing the use made of the work. Further, any new works must be made available on the same conditions. The full details of the license are available at <http://creativecommons.org/licenses/by-nc-sa/4.0>.

**CC BY NC ND:** The CC BY-NC-ND license allows users to copy and distribute the Article, provided this is not done for commercial purposes and further does not permit distribution of the Article if it is changed or edited in any way, and provided the user gives appropriate credit (with a link to the formal publication through the relevant DOI), provides a link to the license, and that the licensor is not represented as endorsing the use made of the work. The full details of the license are available at <http://creativecommons.org/licenses/by-nc-nd/4.0>.

Any commercial reuse of Open Access articles published with a CC BY NC SA or CC BY NC ND license requires permission from Elsevier and will be subject to a fee.

Commercial reuse includes:

- Associating advertising with the full text of the Article
- Charging fees for document delivery or access
- Article aggregation
- Systematic distribution via e-mail lists or share buttons

Posting or linking by commercial companies for use by customers of those companies.

## 20. Other Conditions:

v1.9

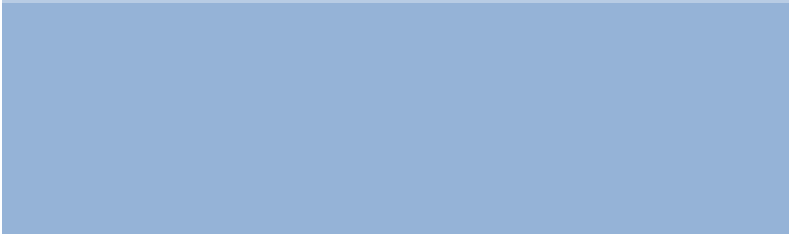
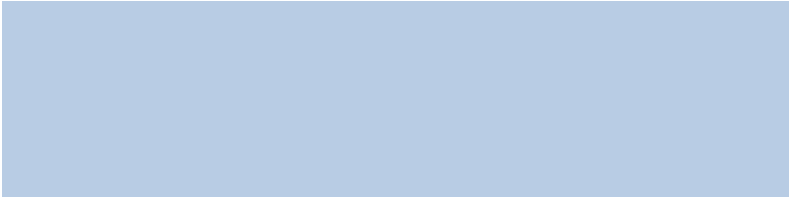
**Questions?** [customercare@copyright.com](mailto:customercare@copyright.com) or +1-855-239-3415 (toll free in the US) or +1-978-646-2777.



$\gamma$ H2AX total    $\gamma$ H2AX G1    $\gamma$ H2AX S    $\gamma$ H2AX G2    $\gamma$ H2AX M



$\gamma$ H2AX total    $\gamma$ H2AX G1    $\gamma$ H2AX S    $\gamma$ H2AX G2    $\gamma$ H2AX M



## Treatment 1

Sample	subG1	G1	S	G2	M	Sum	G1_DJF	S_DJF	G2/M_DJF	Sum
control1_t1-1	#####	####	####	####	###	#####	#DIV/0!	#DIV/0!	#DIV/0!	#####
control1_t1-2	#####	####	####	####	###	#####	#DIV/0!	#DIV/0!	#DIV/0!	#####
control1_t1-3	#####	####	####	####	###	#####	#DIV/0!	#DIV/0!	#DIV/0!	#####
treatment1_t1-1	#####	####	####	####	###	#####	#DIV/0!	#DIV/0!	#DIV/0!	#####
treatment1_t1-2	#####	####	####	####	###	#####	#DIV/0!	#DIV/0!	#DIV/0!	#####
treatment1_t1-3	#####	####	####	####	###	#####	#DIV/0!	#DIV/0!	#DIV/0!	#####
control1_t2-1	#####	####	####	####	###	#####	#DIV/0!	#DIV/0!	#DIV/0!	#####
control1_t2-2	#####	####	####	####	###	#####	#DIV/0!	#DIV/0!	#DIV/0!	#####
control1_t2-3	#####	####	####	####	###	#####	#DIV/0!	#DIV/0!	#DIV/0!	#####
treatment2_t2-1	#####	####	####	####	###	#####	#DIV/0!	#DIV/0!	#DIV/0!	#####
treatment2_t2-2	#####	####	####	####	###	#####	#DIV/0!	#DIV/0!	#DIV/0!	#####
treatment2_t2-3	#####	####	####	####	###	#####	#DIV/0!	#DIV/0!	#DIV/0!	#####

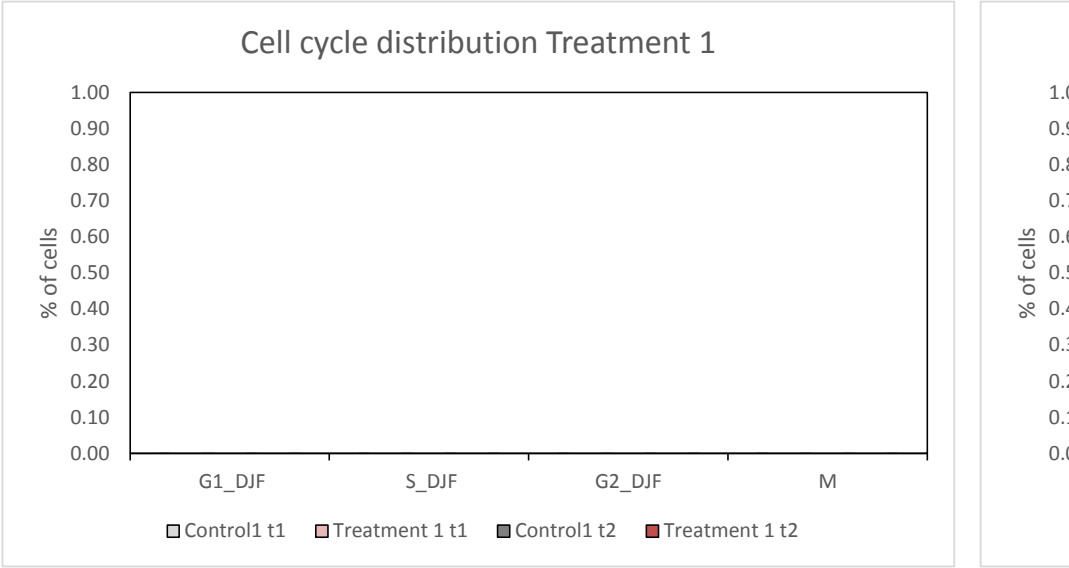
## Treatment 2

Sample	subG1	G1	S	G2	M	Sum	G1_DJF	S_DJF	G2/M_DJF	Sum
control2_t1-1	#####	####	####	####	###	#####	#DIV/0!	#DIV/0!	#DIV/0!	#####
control2_t1-2	#####	####	####	####	###	#####	#DIV/0!	#DIV/0!	#DIV/0!	#####
control2_t1-3	#####	####	####	####	###	#####	#DIV/0!	#DIV/0!	#DIV/0!	#####
treatment2_t1-1	#####	####	####	####	###	#####	#DIV/0!	#DIV/0!	#DIV/0!	#####
treatment2_t1-2	#####	####	####	####	###	#####	#DIV/0!	#DIV/0!	#DIV/0!	#####
treatment2_t1-3	#####	####	####	####	###	#####	#DIV/0!	#DIV/0!	#DIV/0!	#####
control2_t2-1	#####	####	####	####	###	#####	#DIV/0!	#DIV/0!	#DIV/0!	#####
control2_t2-2	#####	####	####	####	###	#####	#DIV/0!	#DIV/0!	#DIV/0!	#####
control2_t2-3	#####	####	####	####	###	#####	#DIV/0!	#DIV/0!	#DIV/0!	#####
treatment2_t2-1	#####	####	####	####	###	#####	#DIV/0!	#DIV/0!	#DIV/0!	#####
treatment2_t2-2	#####	####	####	####	###	#####	#DIV/0!	#DIV/0!	#DIV/0!	#####
treatment2_t2-3	#####	####	####	####	###	#####	#DIV/0!	#DIV/0!	#DIV/0!	#####



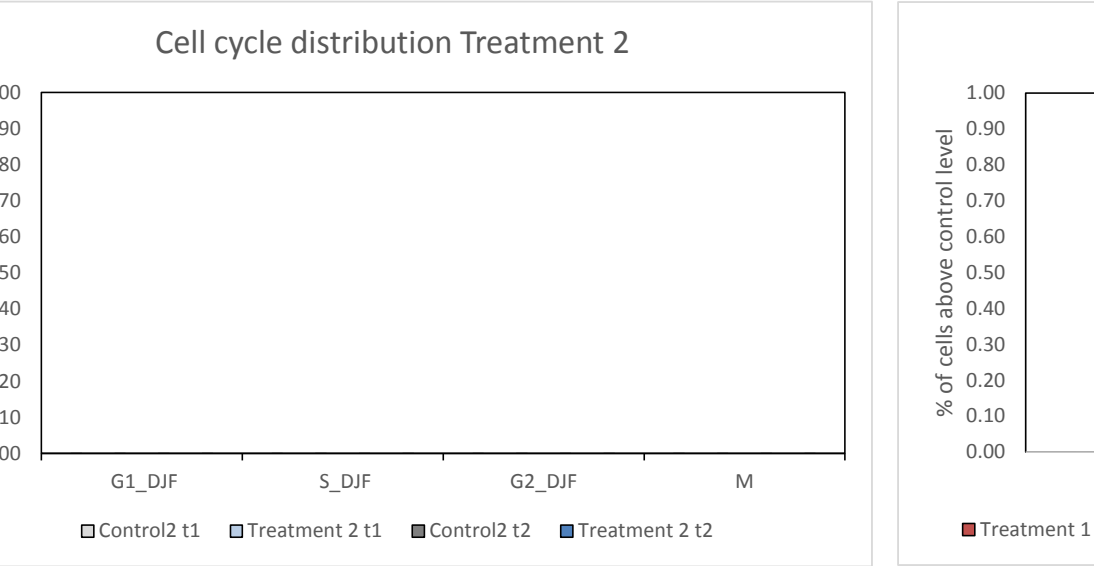


Treatment	Time	Mean	Mean	Mean	Mean	Mean
		subG1	Casp3-A+	G1_DJF	S_DJF	G2_DJF
Control1	t1	#DIV/0!	#DIV/0!	#DIV/0!	#DIV/0!	#DIV/0!
Treatment 1	t1	#DIV/0!	#DIV/0!	#DIV/0!	#DIV/0!	#DIV/0!
Control1	t2	#DIV/0!	#DIV/0!	#DIV/0!	#DIV/0!	#DIV/0!
Treatment 1	t2	#DIV/0!	#DIV/0!	#DIV/0!	#DIV/0!	#DIV/0!
Control2	t1	#DIV/0!	#DIV/0!	#DIV/0!	#DIV/0!	#DIV/0!
Treatment 2	t1	#DIV/0!	#DIV/0!	#DIV/0!	#DIV/0!	#DIV/0!
Control2	t2	#DIV/0!	#DIV/0!	#DIV/0!	#DIV/0!	#DIV/0!
Treatment 2	t2	#DIV/0!	#DIV/0!	#DIV/0!	#DIV/0!	#DIV/0!



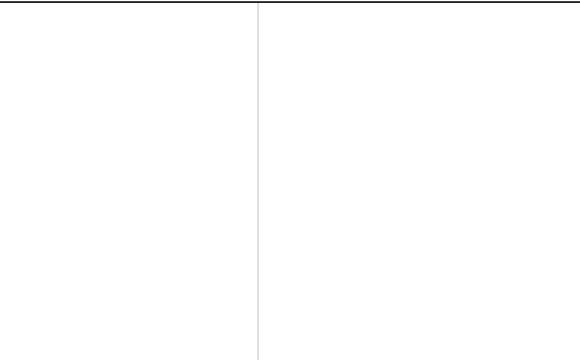


Mean	SD	SD	SD	SD	SD	SD
M	subG1	Casp3-A+	G1_DJF	S_DJF	G2_DJF	M
#DIV/0!	#DIV/0!	#DIV/0!	#DIV/0!	#DIV/0!	#DIV/0!	#DIV/0!
#DIV/0!	#DIV/0!	#DIV/0!	#DIV/0!	#DIV/0!	#DIV/0!	#DIV/0!
#DIV/0!	#DIV/0!	#DIV/0!	#DIV/0!	#DIV/0!	#DIV/0!	#DIV/0!
#DIV/0!	#DIV/0!	#DIV/0!	#DIV/0!	#DIV/0!	#DIV/0!	#DIV/0!
#DIV/0!	#DIV/0!	#DIV/0!	#DIV/0!	#DIV/0!	#DIV/0!	#DIV/0!
#DIV/0!	#DIV/0!	#DIV/0!	#DIV/0!	#DIV/0!	#DIV/0!	#DIV/0!
#DIV/0!	#DIV/0!	#DIV/0!	#DIV/0!	#DIV/0!	#DIV/0!	#DIV/0!
#DIV/0!	#DIV/0!	#DIV/0!	#DIV/0!	#DIV/0!	#DIV/0!	#DIV/0!



<i>t test</i>	<i>t test</i>	<i>t test</i>	<i>t test</i>	<i>t test</i>	<i>t test</i>
subG1	Casp3-A+	G1_DJF	S_DJF	G2_DJF	M
#DIV/0!	#DIV/0!	#DIV/0!	#DIV/0!	#DIV/0!	#DIV/0!
#DIV/0!	#DIV/0!	#DIV/0!	#DIV/0!	#DIV/0!	#DIV/0!
		#DIV/0!	#DIV/0!	#DIV/0!	#DIV/0!
		#DIV/0!	#DIV/0!	#DIV/0!	#DIV/0!
		#DIV/0!	#DIV/0!	#DIV/0!	#DIV/0!

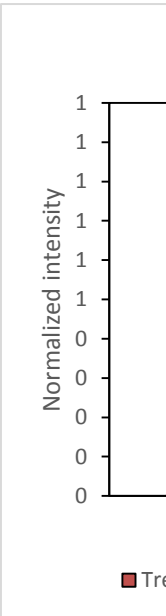
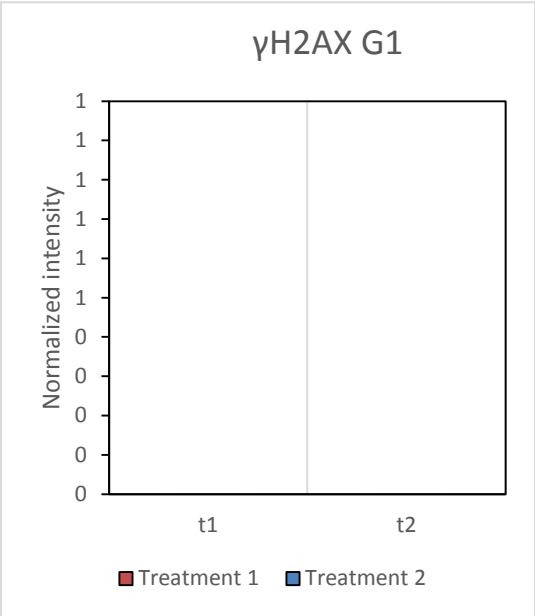
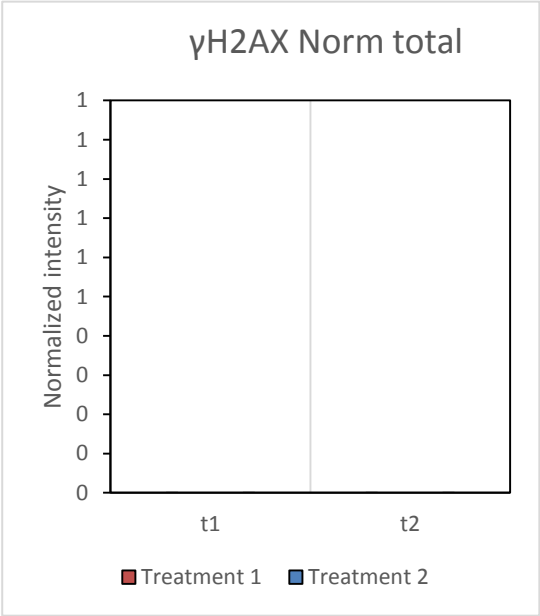
Apoptosis



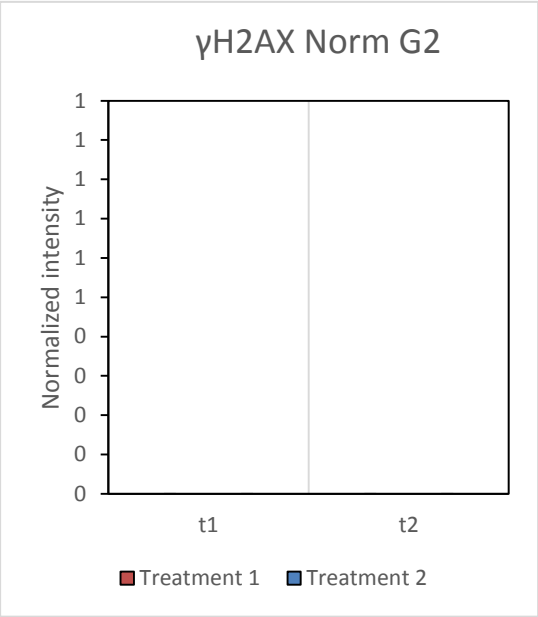
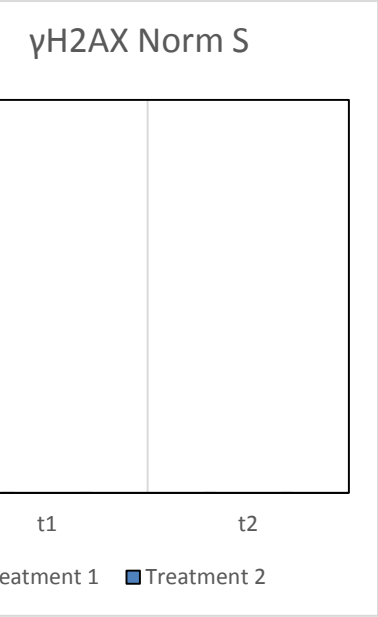
subG1                      Casp3-A+

t1   ■ Treatment 2 t1   ■ Treatment 1 t2   ■ Treatment 2 t2

Treatment	Time	Mean	Mean	Mean	Mean	Mean	SD
		γH2AX Norm	γH2AX G1	γH2AX Norm	γH2AX Norm	γH2AX Norm	γH2AX Norm
Treatment 1	t1	#DIV/0!	0.00	0.00	0.00	0.00	#DIV/0!
Treatment 1	t2	#DIV/0!	0.00	0.00	0.00	0.00	#DIV/0!
Treatment 2	t1	#DIV/0!	0.00	0.00	0.00	0.00	#DIV/0!
Treatment 2	t2	#DIV/0!	0.00	0.00	0.00	0.00	#DIV/0!



SD	SD	SD	SD	t test	t test	t test	t test
γH2AX G1	γH2AX Norm	γH2AX Norm	γH2AX Norm	γH2AX Norm	γH2AX G1	γH2AX Norm	γH2AX Norm
0.00	0.00	0.00	0.00	0.00	#DIV/0!	#DIV/0!	#DIV/0!
0.00	0.00	0.00	0.00	0.00	#DIV/0!	#DIV/0!	#DIV/0!
0.00	0.00	0.00	0.00	0.00			
0.00	0.00	0.00	0.00	0.00			



*t test*

**γH2AX Norm M**

#DIV/0!

#DIV/0!

